JACC: CARDIOVASCULAR IMAGING VOL. 18, NO. 4, 2025

STATE-OF-THE-ART REVIEW

The Last Decade in Cardiac Amyloidosis

Advances in Understanding Pathophysiology, Diagnosis and Quantification, Prognosis, Treatment Strategies, and Monitoring Response

Marianna Fontana, MD, PhD,[a,*] Adam Ioannou, MBBS, BSc, PhD,[a,*] Sarah Cuddy, MBBCH, BAO,[b] Sharmila Dorbala, MD, MPH,[b] Ahmad Masri, MD,[c] James C. Moon, MD,[d] Vasvi Singh, MD,[b] Olivier Clerc, MD,[b] Mazen Hanna, MD,[e] Fredrick Ruberg, MD,[f] Martha Grogan, MD,[g] Michele Emdin, MD, PhD,[h,i] Julian Gillmore, MD, PhD[a]

ABSTRACT

Cardiac amyloidosis represents a unique disease process characterized by amyloid fibril deposition within the myocardial extracellular space. Advances in multimodality cardiac imaging enable accurate diagnosis and facilitate prompt initiation of disease-modifying therapies. Furthermore, rapid advances in multimodality imaging have enriched understanding of the underlying pathogenesis, enhanced prognostication, and resulted in the development of imaging-based markers that reflect the amyloid burden, which is of increasing importance when assessing the response to treatment. Whereas conventional therapies have focused on reducing amyloid formation and subsequent stabilization of the cardiac disease process, novel agents are being developed to accelerate the immune-mediated removal of amyloid fibrils from the heart. In this context, the ability to track changes in the amyloid burden over time is of paramount importance. Although advanced imaging techniques have shown efficacy in tracking the treatment response, future research focused on improved precision through use of artificial intelligence may augment the detection of changes earlier in the course of treatment. (JACC Cardiovasc Imaging. 2025;18:478-499) © 2025 The Authors. Published by Elsevier on behalf of the American College of Cardiology Foundation. This is an open access article under the CC BY-NC-ND license (http://creativecommons.org/licenses/by-nc-nd/4.0/).

Amyloidosis is a clinical disease process characterized by the deposition of amyloid fibrils within the extracellular space of various organs. Amyloid fibrils are formed when proteins with an unstable tertiary structure misfold into insoluble beta-pleated sheets, resistant to proteolysis, that subsequently aggregate and deposit within the extracellular matrix. Disease occurs when the accumulation of amyloid fibrils disrupts the structure, integrity, and function of the affected organ.[1]

Cardiac amyloidosis (CA) occurs when amyloid fibrils accumulate within the myocardium, causing interruption and distortion of myocardial contractile elements. The overwhelming majority of CA cases

From the [a]National Amyloidosis Centre, University College London, Royal Free Campus, Rowland Hill Street, London, United Kingdom; [b]Department of Medicine and Radiology, CV Imaging Program, Cardiovascular Division, Brigham and Women's Hospital and Harvard Medical School, Boston, Massachusetts, USA; [c]OHSU Center for Hypertrophic Cardiomyopathy and Amyloidosis, Portland, Oregon, USA; [d]Institute of Cardiovascular Science, University College London, United Kingdom; [e]Department of Cardiovascular Medicine, Amyloidosis Center, Cleveland Clinic, Cleveland, Ohio, USA; [f]Section of Cardiovascular Medicine, Department of Medicine, Amyloidosis Center, Boston University School of Medicine, Boston Medical Center, Boston, Massachusetts, USA; [g]Department of Cardiovascular Diseases, Mayo Clinic, Rochester, Minnesota, USA; [h]Health Science Interdisciplinary Center, Scuola Superiore Sant'Anna, Pisa, Italy; and the [i]Fondazione Toscana Gabriele Monasterio, Pisa, Italy. *These authors contributed equally to this work.

The authors attest they are in compliance with human studies committees and animal welfare regulations of the authors' institutions and Food and Drug Administration guidelines, including patient consent where appropriate. For more information, visit the Author Center.

Manuscript received August 29, 2024; revised manuscript received October 3, 2024, accepted October 11, 2024.

ISSN 1936-878X https://doi.org/10.1016/j.jcmg.2024.10.011

result from misfolded light-chain (light-chain amyloidosis [AL]) and transthyretin (transthyretin amyloidosis [ATTR]) proteins,[2,3] although less common causes such as apolipoprotein AI amyloidosis (AApoAI) and apolipoprotein AIV amyloidosis (AApoAIV) are increasingly being recognized.[4] Despite differences in prevalence, clinical phenotype, prognosis, and treatment strategies across this heterogenous group of diseases, cardiac involvement is consistently the leading cause of morbidity and mortality.[2-4]

Systemic AL amyloidosis occurs as the result of deposition of misfolded monoclonal immunoglobulin light-chains, produced by an abnormal clonal proliferation of plasma cells. AL-amyloid fibrils can infiltrate multiple different organs; therefore, the disease can present with a wide array of signs and symptoms. The nonspecific clinical presentation, coupled with a limited index of suspicion outside of specialist centers, often results in a delayed diagnosis, which, in the context of cardiac involvement, can have devastating consequences with a median survival of 6 months in patients with advanced cardiac disease without treatment.[1]

Transthyretin (TTR) is a tetrameric protein that participates in the plasma transport of both thyroxine and retinol. It is synthesized by the liver and by choroid plexus and disease occurs when it dissociates into oligomers and monomers that subsequently misfold into pathogenic ATTR-amyloid insoluble fibrils. In vivo fragmentation of TTR by endogenous proteases has also been implicated in the formation of amyloid fibrils. Aberrant proteolysis results in the formation of large fragments that are more unstable than the parent protein and display a greater tendency to form self-aggregating intermediates that subsequently form amyloid fibrils.[3] The misfolding can occur secondary to an inherited, autosomal dominant single point mutation in the TTR gene, known or variant (ATTRv), or via an acquired process associated with aging through unknown exact mechanism known as wild-type ATTR (wtATTR). wtATTR is a condition of older, predominantly male individuals; whereas ATTRv presents at various ages depending on the specific mutation, with either a prevalent neuropathic, cardiac, or a mixed clinical phenotype comprised of a cardiomyopathy and length-dependent, small fiber, peripheral sensorimotor, and autonomic neuropathy. TTR variants are endemic to certain areas with the p.(Val50Met) variant being most common in Europe and the p.(Val142Ile) variant thought to be carried by up to 3% to 4% of African Americans.[5,6] In contrast to systemic AL amyloidosis, in ATTR-CA disease progression occurs at a slower rate, with a median survival of 3 to 5 years without treatment.[7]

The recognition of ATTR-CA, and in particular wtATTR-CA, has increased substantially in recent years. Increasing awareness among clinicians, coupled with advancements in multimodality cardiac imaging techniques, has resulted in a dramatic increase in diagnoses, with ATTR-CA accounting for 6% to 16% of older patients presenting with heart failure and increased left ventricular (LV) wall thickness, as well as concurrently identified in those undergoing valve replacement for severe aortic stenosis.[8-11]

Improvements in multimodality cardiac imaging has not only augmented diagnostics but also enhanced our understanding of the underlying pathophysiology, enabled more accurate assessments of an individual's CA burden, and aided prognostication with development toward disease progression and therapeutic efficacy.

ABBREVIATIONS AND ACRONYMS

AL-CA = light-chain cardiac amyloidosis

ATTR-CA = transthyretin cardiac amyloidosis

CA = cardiac amyloidosis

CMR = cardiac magnetic resonance

ECV = extracellular volume

FLC = free light chains

LGE = late gadolinium enhancement

LV = left ventricular

PET = positron emission tomography

DIAGNOSIS AND QUANTIFICATION OF THE AMYLOID BURDEN

ECHOCARDIOGRAPHY. Echocardiography is the most widely available cardiac imaging modality. It is uniquely positioned to characterize cardiac structure while simultaneously assessing systolic and diastolic function; thus, it represents a crucial first-line investigation in patients with heart failure. CA is characterized by biventricular wall thickening and stiffening of the myocardium resulting in impaired relaxation (**Figure 1**). Hence, CA is often conceived as heart failure with preserved ejection fraction; however, this classification underestimates the degree of systolic impairment that occurs during amyloid infiltration.[3] Amyloid fibril deposition occurs from the base to apex, and from the endocardium to epicardium. Longitudinal contractile myocardial fibers are predominantly situated in the endocardium, whereas radial contractile fibers are positioned in the midwall. Therefore, longitudinal contraction becomes impaired early in the disease process, whereas radial contraction is preserved until end-stage.[12] The pattern of infiltration often results in an apical sparing longitudinal strain pattern, increasing suspicion for the diagnosis. Apical sparing can be present in aortic stenosis and other hypertrophic conditions, and the sensitivity and specificity varies depending on the cohort of patients examined; eg, it has been shown to have a lower specificity in patients with chronic kidney disease.[13,14] Alternative measures

JACC: CARDIOVASCULAR IMAGING, VOL. 18, NO. 4, 2025
APRIL 2025:478–499

FIGURE 1 Typical Echocardiographic Features of a Patient With Cardiac Transthyretin Amyloidosis

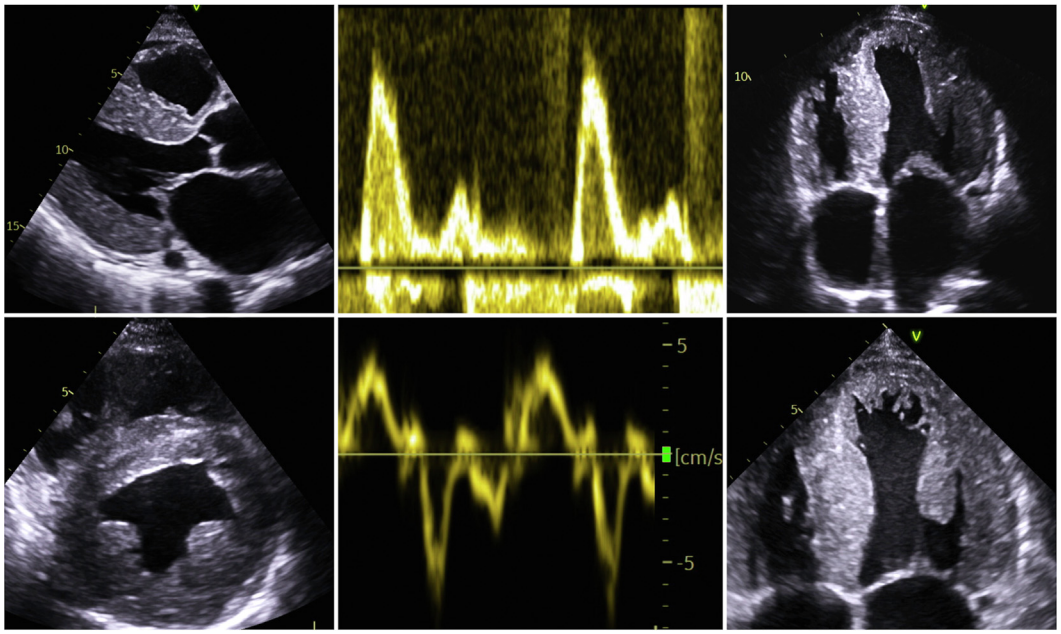

such as the septal apical-to-base ratio have shown an improved diagnostic accuracy[15] and, when combined with other features associated with CA, it can yield a specificity of up to 98%.[16] Longitudinal strain is a reproducible metric and has been proposed as a metric to track disease progression; however, strain metrics that incorporate blood pressure, including myocardial work index and efficiency, deteriorate to a greater degree than longitudinal strain in untreated patients and are independently prognostic.[17]

There is a growing body of published reports harnessing individual echocardiographic metrics or a combination of metrics to develop scoring systems that enhance diagnostic capabilities. Initial studies of apical sparing strain ratios were conducted in select populations;[18] when evaluated in less select populations, the high sensitivity and specificity of the initial thresholds was not reproduced.[19] Models that include a combination of either clinical or echocardiographic metrics have areas under the curve (AUCs) >0.8, but they lack a single threshold with both high sensitivity and specificity. Machine learning offers the opportunity to move beyond conventional statistical models and has shown great promise for automated detection of CA based on standard images.[20]

More recently, the effects of atrial amyloid infiltration have been appreciated. Left atrial strain assessments have shown a progressive loss of atrial function and increased atrial stiffness. Extensive amyloid infiltration of the atria results in a loss of normal atrial contraction, even in the context of sinus rhythm, a phenomenon also known as atrial electromechanical dissociation.[21] The effects of reduced cardiac output along with direct atrial amyloid infiltration causes blood stasis and an increased prevalence of atrial thrombi, even in the presence of anticoagulation.[22]

Valvular abnormalities have also been extensively described in CA, with concomitant aortic stenosis and mitral and tricuspid regurgitation being particularly common and associated with a worse prognosis.[23] Additionally, worsening of the degree of regurgitation over time is also associated with a worse prognosis.[24]

There are structural and functional differences between the various forms of CA, with ATTR-CA often presenting with a greater biventricular mass, and more asymmetrical septal thickening than AL-CA. Whereas AApoAI can present with disproportionate right-sided involvement with a greater incidence of tricuspid valve dysfunction, a significant overlap in echocardiographic phenotype still exists, making echocardiographic features alone unsuited to differentiate the different types.[4,25]

SERUM AMYLOID P COMPONENT SCINTIGRAPHY

This nuclear imaging technique involves administration of ^{123}I-labeled purified human serum amyloid P

FIGURE 2 Serum Amyloid P Scintigraphy Images Showing Evidence of Organ Regression in Patients With Systemic Amyloid a Amyloidosis and Systemic Light Chain Amyloidosis

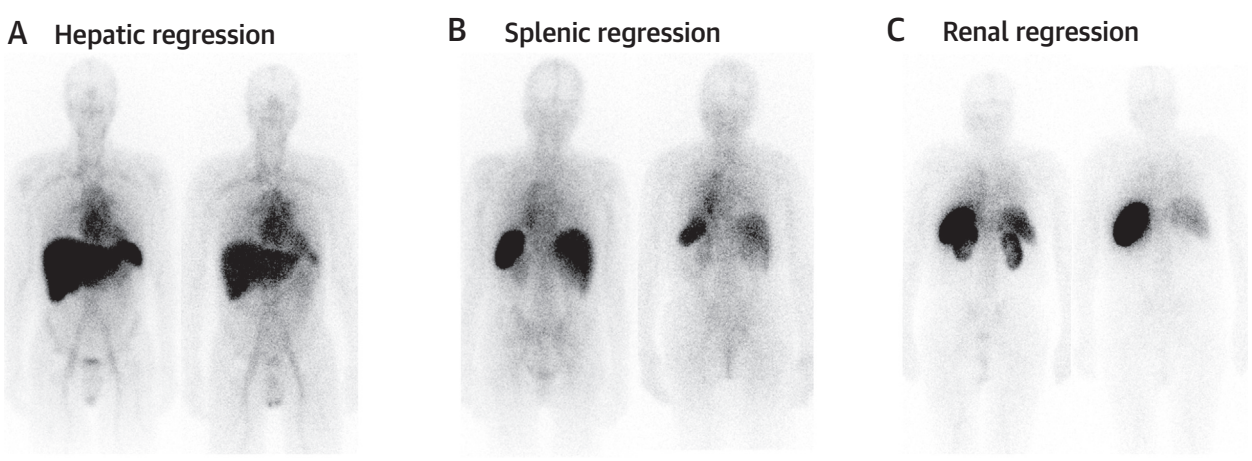

(A) Hepatic regression. (B) Splenic regression. (C) Renal regression.

component (SAP), which has a high binding affinity to amyloid fibrils, and following gamma camera acquisition allows accurate quantification of the hepatic, splenic, and renal amyloid load but cannot assess the presence of myocardial infiltration. Following corroboration with biopsy samples, the images obtained identify amyloid accumulation in the visceral organs with a high degree of sensitivity and specificity.[26] Serial SAP scintigraphy scans enable direct visualization of the dynamic turnover of amyloid deposits in response to treatment and demonstrated, for the first time, that a substantial reduction in the amyloid precursor protein in patients with systemic AA amyloidosis and systemic AL amyloidosis often leads to gradual disease regression in the visceral organs. This discovery occurred over 2 decades ago and was the first demonstration of disease regression in patients with systemic amyloidosis (**Figure 2**).[26]

CARDIAC MAGNETIC RESONANCE. Cardiac magnetic resonance (CMR) provides similar structural and functional information to echocardiography, with additional information regarding tissue composition through tissue characterization, thereby enabling CMR to help differentiate CA from other causes of a hypertrophic phenotype. Use of gadolinium-based contrast agents has formed the cornerstone of diagnostics, and late gadolinium enhancement (LGE) imaging often shows typical patterns of subendocardial or transmural enhancement.[27]

The main drawback of LGE imaging is that it is not inherently quantitative; however, this limitation may be overcome with multiparametric mapping. Precontrast native-T1 mapping offers a measure of the myocardial relaxation time that is often elevated in the context of CA, and has shown a high diagnostic accuracy in patients referred to specialist centers with a high pretest probability of CA.[28] However, native-T1 mapping provides a composite signal from the intracellular and extracellular space and does not differentiate the underlying disease process responsible for its elevation.

Administration of gadolinium-based contrast agents enables isolation of the extracellular signal. Amyloidosis is the exemplar interstitial disease; therefore, the extracellular volume (ECV) acts as a surrogate measure of the interstitial amyloid. Elevations in ECV occur early in the disease process, before LGE and changes in cardiac structure and function and, hence, ECV has a high diagnostic accuracy.[27] Using ECV as a surrogate marker of amyloid burden has provided important insights into the underlying amyloid disease process because various structural and functional parameters become abnormal at different ECV thresholds reflective of the burden of deposition. Longitudinal strain becomes abnormal at a low ECV, whereas biventricular ejection fraction only becomes abnormal at a higher ECV, likely reflecting infiltration of subendocardial longitudinal fibers in the earlier stages of the disease (**Figure 3**).[12] ECV can also be used to quantify the myocyte response: detecting differences between AL-CA and ATTR-CA with an apparent relative (compensatory) hypertrophy response in ATTR that is not present in AL. Despite patients with ATTR-CA having a greater

FIGURE 3 CMR Images

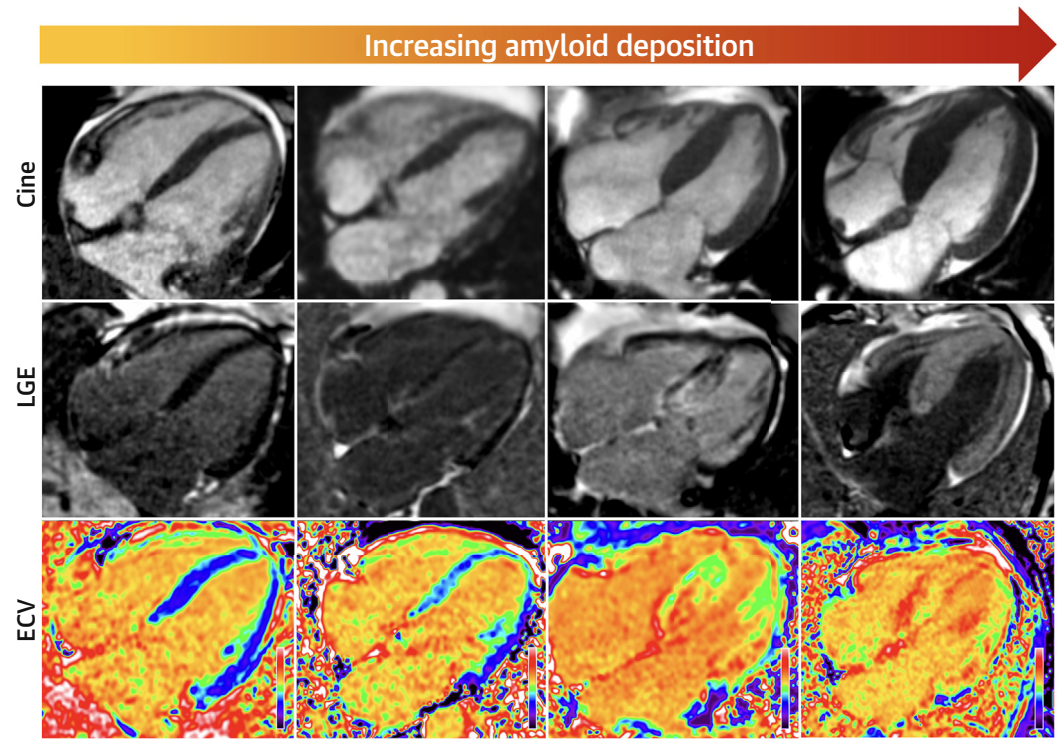

Cardiac magnetic resonance (CMR) images showing an increasing transmurality of late gadolinium enhancement (LGE) and extracellular volume (ECV) as more amyloid fibrils accumulate in the myocardium.

LV mass, increased transmurality of LGE, and higher ECV than patients with AL-CA, these findings are not specific and CMR alone cannot be used to differentiate between different forms of amyloidosis as there is significant imaging overlap.[29]

Routine CMR has also shown high diagnostic performance in detecting hepatic and splenic amyloid infiltration, which is of particular importance in systemic AL amyloidosis, whereby, multiorgan involvement is common. The diagnostic performance of measuring liver and spleen ECV has been compared with SAP scintigraphy. There is good correlation between the 2 imaging modalities, and significant ECV elevations detect visceral organ involvement with a high degree of accuracy, which not only helps refine the diagnostic differentials but also has important implications with regards to treatment decisions.[30]

Mapping techniques have dramatically increased our understanding of the underlying pathogenesis in CA. T2 mapping serves as a surrogate marker for myocardial edema. Following corroboration with histologic samples, this noninvasive technique was able to show that myocardial edema occurs in AL-CA, presumably because of the impact of direct light-chain toxicity and resultant myocardial injury.[31]

Quantitative stress perfusion mapping has shown that patients with CA have a severely reduced stress myocardial blood flow, which is similar to patients with triple-vessel coronary disease. Perfusion abnormalities correlated with markers of amyloid burden and were corroborated with endomyocardial biopsy specimens, which showed amyloid infiltration at the level of mural arterioles and disruption and refraction of the capillaries, with hypoxic conditions resulting in upregulation of vascular endothelial growth factor.[32]

When combined, CMR structure, function, LGE, and mapping enable redefinition of cardiac involvement through disease processes: 1) amyloid burden with ECV; 2) edema with T2; 3) ischemia with perfusion mapping; 4) myocyte response (derived from: LV mass $\times$ [1-ECV]); and 5) disease severity through a combination of LGE and ECV. Advances in multiparametric mapping have not only improved the diagnostic accuracy of CMR but also enriched the understanding of the underlying disease process and enabled noninvasive measurements of the CA burden.

FIGURE 4 Cardiac Scintigraphy Images

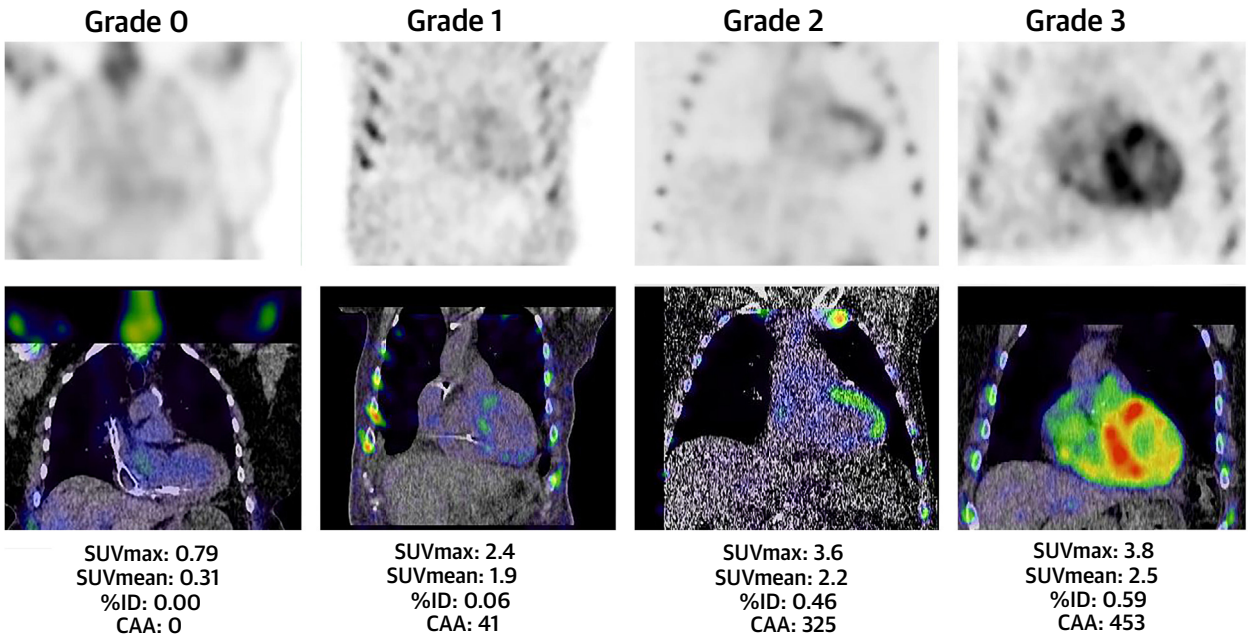

Cardiac scintigraphy images with ^{99m}technetium-labelled pyrophosphate of a patient with varying degrees of myocardial radiotracer uptake. %ID = percentage injected dose; CAA = cardiac amyloid activity; SUV = standardized uptake value.

CARDIAC SCINTIGRAPHY WITH BONE AVID RADIOTRACERS. Bone scintigraphy was first repurposed in the 1980s, following the incidental finding of myocardial uptake of technetium-based bone-avid radiotracers in patients with CA. A seminal study showed the diagnostic potential of ^{99m}technetium-labelled 3,3-dicarboxypropane-2, 1-diphosphonate (^{99m}Tc-DPD) in identifying ATTR-CA, based on a visual score of the cardiac uptake seen on planar images (grade 0 = absent cardiac uptake; grade 1 = mild uptake < bone; grade 2 = moderate uptake equal to bone; and grade 3 = high uptake > bone) (**Figure 4**).[33] Subsequent studies have confirmed the utility of multiple different bone-avid radiotracers in the detection of ATTR-CA (^{99m}Tc-hydroxymethylene diphosphonate [^{99m}Tc-HMDP)], and ^{99m}Tc-pyrophosphate [^{99m}Tc-PYP]).[34] However, it is increasingly recognized that myocardial radiotracer uptake can also occur in other forms of CA, with rarer forms such as AApoAI and AApoAIV presenting with mild (grade 1) cardiac uptake, and up to 40% of patients with AL-CA presenting with cardiac radiotracer uptake.[4,35,36] These observations led to a new diagnostic algorithm for ATTR-CA, which used the impressive sensitivity of cardiac scintigraphy alongside serum free light chains (FLCs) and serum and urine immunofixation electrophoresis to exclude systemic AL amyloidosis.

The ground-breaking study that resulted in widespread use of bone-avid tracer cardiac scintigraphy establishing the nonbiopsy pathway for ATTR-CA showed the presence of grade 2-3 myocardial radiotracer uptake conferred a sensitivity of >99% and specificity of 86% for ATTR-CA, with most false positives occurring in patients with AL-CA. The combination of a positive scan with the absence of monoclonal proteins by serum and urine testing (thereby excluding systemic AL amyloidosis) improved the specificity to 100%, but, due to the high prevalence of a monoclonal gammopathy in this elderly population, this also resulted in a reduction in the sensitivity to 70%.[36] The diagnostic algorithm has since been validated in several studies, including a large multicenter study which confirmed a high specificity and positive predictive value of the nonbiopsy pathway.[37]

Despite the high diagnostic accuracy, some questions remain unanswered. The aforementioned studies have used cardiac scintigraphy with bone-avid radiotracers in patients with a high clinical suspicion of CA.[36,37] The high performance in diagnosing

ATTR-CA has been favorably skewed because of the high prevalence of cases and pretest probability in study cohorts. It is likely that application to populations with a lower prevalence and less severe disease would result in a reduced positive predictive value.[34]

In patients with wtATTR-CA, grade 1 (mild) uptake can represent an early disease marker, which precedes the onset of structural and functional cardiac abnormalities.[25] In contrast, certain hereditary variants, such as Ser77Tyr, Tyr114Cys, and Phe64Leu, present with disproportionately low myocardial radiotracer uptake (ie, no uptake or mild uptake) despite associated heart failure symptoms and characteristic imaging on echocardiography and CMR; hence, they do not fulfil the nonbiopsy diagnostic criteria.[25] If a strong clinical suspicion remains following a scan showing no uptake or mild uptake, sequencing of the *TTR* gene and CMR should be considered to reduce the risk of misdiagnosis.

Nevertheless, the majority of patients presenting with a characteristic amyloid CMR and either no uptake or mild cardiac uptake are subsequently diagnosed with AL-CA. Therefore, following the exclusion of rare TTR variants and rare forms of CA through comprehensive genotyping, the combination of a CMR that is characteristic for CA and grade 0 or 1 cardiac uptake on scintigraphy confers a 100% specificity for AL-CA and can be used to refine the diagnostic differentials while awaiting histologic confirmation.[25]

Since the publication of the nonbiopsy pathway, use of bone scintigraphy to diagnose ATTR-CA has risen significantly, with multiple different technetium-based radiotracers being used. The diagnostic performance of these agents is assumed to be broadly similar; however, this hypothesis is yet to be tested in a head-to-head trial. It is possible that optimal image acquisition time and image interpretation techniques may vary between tracers. In the United States, ^{99m}Tc-PYP is most commonly used and scans are predominantly interpreted by nuclear cardiologists; whereas in Europe, ^{99m}Tc-DPD and ^{99m}Tc-HMDP are most commonly used and scans are predominantly interpreted by nuclear medicine physicians. Aside from the conventional visual score, quantitative scores derived from planar imaging have been used in the past. The heart-to-whole-body ratio is used for ^{99m}Tc-DPD and ^{99m}Tc-HMDP, whereas the heart-to-contralateral ratio is used for ^{99m}Tc-PYP; therefore, thoracic imaging may be acquired when using ^{99m}Tc-PYP, whereas whole body imaging is acquired when using ^{99m}Tc-DPD and ^{99m}Tc-HMDP.[38] However, these planar imaging-derived metrics are no longer recommended by the American Society of Nuclear Cardiology for the diagnosis of ATTR-CA in isolation, and visual grading by single-photon emission computed tomography (SPECT) is mandated (SPECT-computed tomography [CT] if available may be preferred). SPECT images are able to differentiate blood pool activity (false positive on planar) from true LV myocardial uptake (true positive) (**Figure 5**).[39] When the recommended imaging methodology is used, there is excellent interobserver reproducibility and intraobserver repeatability of ^{99m}Tc-PYP visual scan interpretation.[40] It is also hypothesized that the magnitude of myocardial radiotracer uptake, as quantified by these various methods, could reflect the CA burden. However, because of competitive tracer uptake, the dynamics and kinetics of radiotracer uptake are significantly influenced by uptake in the bones, soft tissues, skeletal muscle, and the heart. The presence of extracardiac amyloid would influence the percentage cardiac uptake; therefore, this may not be an accurate representation of the CA burden. In the era before availability of TTR-specific therapy, ^{99m}Tc-PYP planar visual grade did not change after ~1.5 years despite clinical evidence of disease progression.[41] In contrast, with use of TTR-directed therapies, emerging data show significant reduction in myocardial uptake of bone-avid tracers despite absence of significant changes in cardiac structure and cardiac function.[42,43] This discordance with structural and functional imaging suggests that a decrease in bone-avid tracer myocardial uptake may represent a molecular change in amyloid fibril rather than a reduction in amyloid mass.

Contemporary research has focused the benefit of pursuing SPECT/CT to allow absolute quantification of the tracer uptake and automating this process using deep learning methods. There is uncertainty whether these metrics can accurately track disease progression, but they may enhance diagnostic accuracy, especially in differentiating grade 1 and 2 cardiac uptake. Future studies are needed to determine whether quantitative measures of radiotracer uptake correlate with established markers of disease and prognosis to further clarify the role of bone scintigraphy in quantifying amyloid burden beyond the well-established qualitative visual score.[44]

POSITRON EMISSION TOMOGRAPHY. Several amyloid-binding positron emission tomography (PET) tracers have been evaluated in patients with CA. ^{11}C-Pittsburgh compound B (PIB) detects both ATTR-CA and AL-CA with a high degree of accuracy. This was first demonstrated in a study of 10 patients with CA, all of whom showed uptake, whereas there was no cardiac

FIGURE 5 False Positive Cardiac Scintigraphy Due to Blood Pool Activity

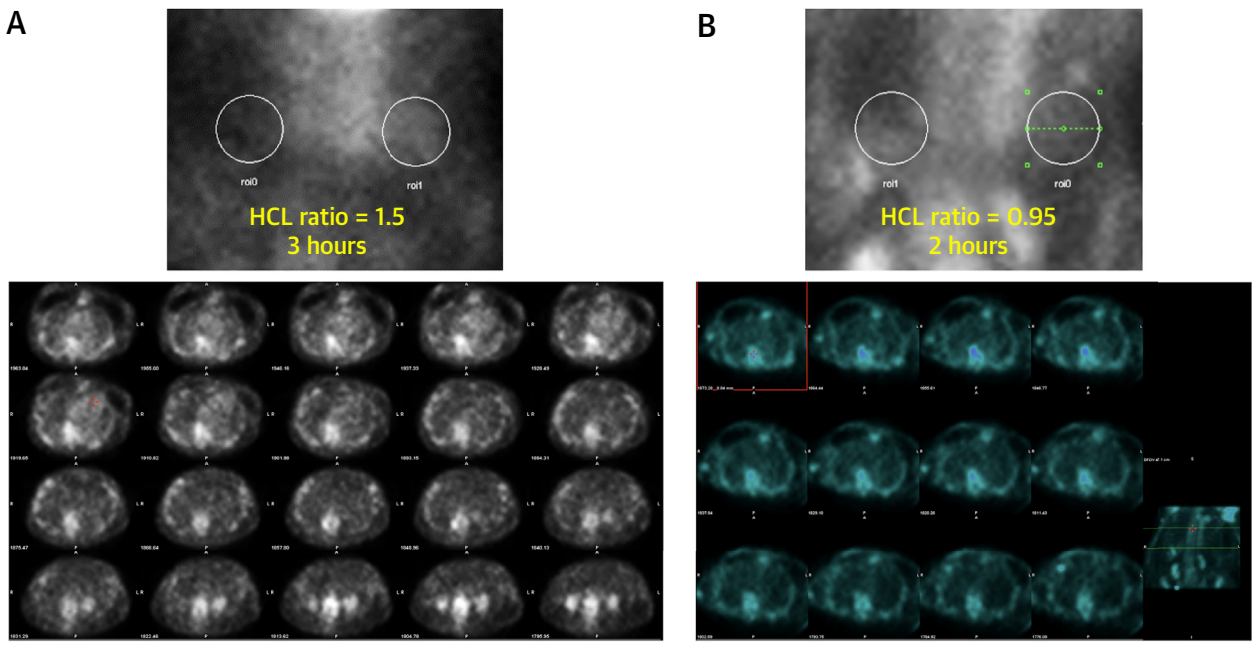

(A) ^{99m}Technetium-labelled pyrophosphate scan showing positive heart-to-contralateral (HCL) lung ratio of 1.5 on planar images. There is significant blood pool activity as is shown on single-photon emission computed tomography (SPECT) images. The HCL lung ratio is a false positive due to residual blood pool activity. (B) The same patient underwent ^{99m}technetium-labelled hydroxydiphosphonate scan that showed a negative HCL lung ratio of 0.95 at 2 hours, and axial SPECT images confirm absence of left ventricular myocardial activity and no significant residual blood pool radiotracer activity (HCL lung ratio also negative).

uptake in 5 healthy controls;[45] this was subsequently confirmed in a small cohort of 15 patients with AL-CA, 13 of whom showed PIB cardiac uptake.[46] However, the requirement for an on-site cyclotron for the production of PIB significantly limits its use.[47] ^{18}F-florbetapir is a stilbene derivative that shows a high binding affinity for amyloid fibrils and has favorable pharmacokinetics with a longer half-life. Ex vivo studies of autopsy-derived myocardial tissue has shown that ^{18}F-florbetapir colocalized well to amyloid deposits,[48] and diagnostic utility has also been confirmed in small in vivo studies of patients with CA.[49] The ^{18}F-florbetapir myocardial uptake (between 4 and 30 minutes) tended to be higher in AL-CA than ATTR-CA but with significant overlap making it challenging to distinguish AL-CA from ATTR-CA.[48] A study of 40 patients with CA (ATTR-CA: 20, AL-CA: 20) using ^{18}F-florbetaben showed that, although all patients exhibited intense early cardiac tracer uptake (5 to 15 minutes), patients with AL-CA showed a higher persistent uptake on the late scan (50 to 60 minutes), whereas in patients with ATTR-CA, myocardial uptake decreased after 15 minutes. These findings suggest that ^{18}F-florbetaben may be able to differentiate the different types as most ^{18}F- and ^{11}C-labelled beta amyloid binding tracers show lower myocardial uptake in ATTR-CA compared to AL-CA.[50]

In the context of systemic AL amyloidosis, ^{18}F-florbetapir has shown utility in detecting early cardiac amyloid infiltration, and the degree of uptake reflects the amyloid burden, with the greatest uptake being observed in patients with established CA and the lowest in those without cardiac involvement, as per the conventional diagnostic criteria.[51] ^{18}F-florbetapir is also able to detect right ventricular cardiac amyloid infiltration with the degree of uptake correlating with right ventricular mass, ejection fraction, and free wall longitudinal strain.[52]

Whole-body PET imaging has the added advantage of imaging extracardiac organs, which is of particular importance in systemic AL amyloidosis. In a study of 40 patients, ^{18}F-florbetapir PET was able to reliably identify extensive organ involvement and, in many instances, detect early organ infiltration before the development of clinical signs and symptoms.[53]

^{124}I-evuzamitide is a novel pan-amyloid radiotracer that binds to amyloid fibrils from multiple different

JACC: CARDIOVASCULAR IMAGING, VOL. 18, NO. 4, 2025
APRIL 2025:478–499

FIGURE 6 **^{18}F-Florbetapir and ^{124}I-Evuzamitide PET/CT Images for a Patient With Cardiac Light Chain Amyloidosis**

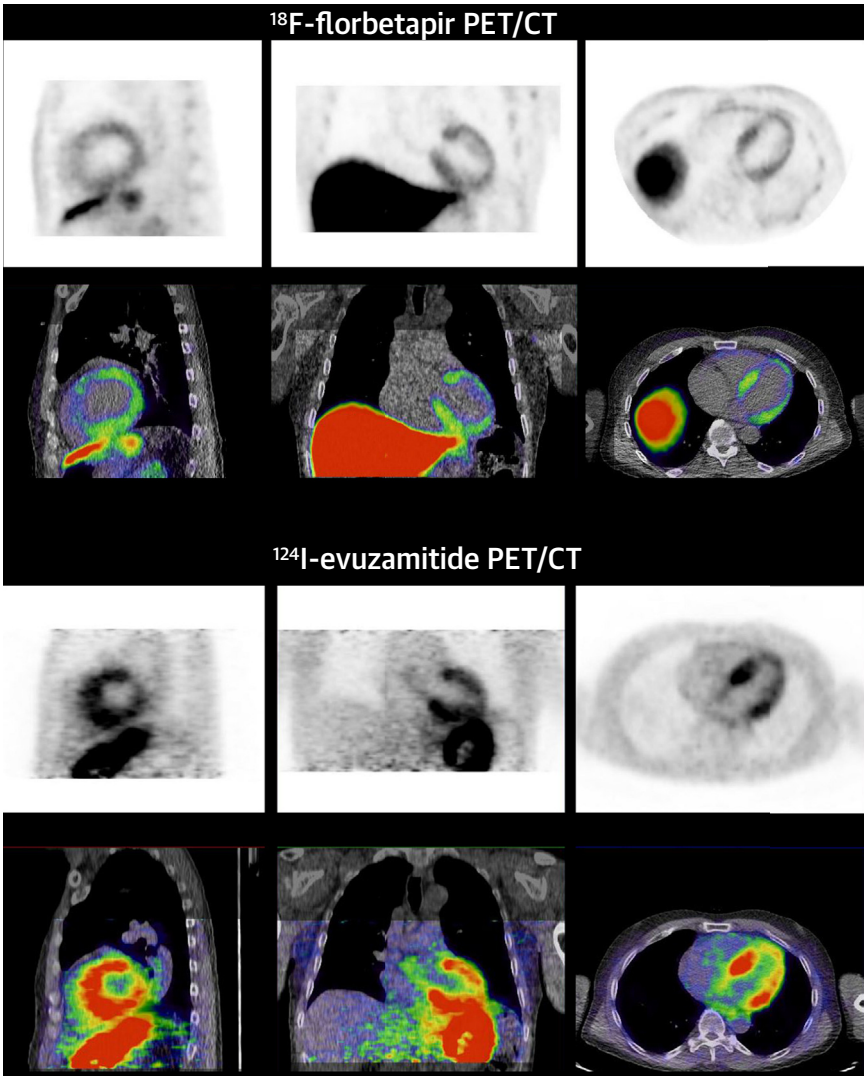

CT = computed tomography; PET = positron emission tomography.

amyloid precursor proteins. In a study of 12 patients with AL-CA and 14 patients with ATTR-CA, cardiac uptake was present in all patients with CA and in none of the healthy control subjects. ^{124}I-evuzamitide possessed a similar diagnostic accuracy to ^{18}F-florbetapir in patients with AL-CA but, in the context of ATTR-CA, there was a greater uptake of ^{124}I-evuzamitide, suggesting that it may possess a superior diagnostic performance. The degree of cardiac uptake correlated well with established markers of disease severity, including CMR derived ECV.[54] Similar to ^{18}F-florbetapir, ^{124}I-evuzamitide has also shown utility in detecting extracardiac infiltration with a high degree of accuracy.[55] However, there are some key differences between the tracers. ^{124}I-evuzamitide can detect liver amyloid but ^{18}F-florbetapir cannot due to physiological uptake. ^{124}I-evuzamitide also undergoes dehalogenation ~4 hours post administration and can be used to image renal amyloid deposition, but it is currently unclear if ^{18}F-florbetapir could be used to detect renal amyloid (**Figure 6**).

Although small studies have shown that various tracers have diagnostic utility, these tracers are still at an early investigational stage, are not reimbursed by 3rd-party payors, and remain not widely accessible. Targeted amyloid-binding PET tracer imaging has a

TABLE 1 Staging Systems Used for Both Cardiac AL Amyloidosis and Cardiac ATTR Amyloidosis

System	NT-proBNP Threshold, ng/L	Troponin-T Threshold, ng/L	Other	Stage
Cardiac AL amyloidosis				
Mayo 2004	332	35		I: both variables below the cutoffs II: 1 variable above the cutoff III: both variables above the cutoff
European modification of Mayo 2004	332 and 8,500	35		I: both variables below the cutoffs II: 1 variable above the cutoff IIIa: NT-proBNP between 332-8,500 ng/L and troponin-T above cutoff IIIb: NT-proBNP >8,500 ng/L and troponin-T above cutoff
Mayo 2012	1,800	25	dFLC: 180 mg/L	I: all below threshold II: 1 above threshold III: 2 above threshold IV: 3 above threshold
Boston University 2019			BNP: 81 ng/L Troponin-I: 10 ng/L	I: both variables below the cutoffs II: 1 variable above the cutoff III: both variables above the cutoff
Cardiac ATTR amyloidosis				
Mayo	3,000	50		I: both variables below the cutoffs II: 1 variable above the cutoff III: both variables above the cutoff
NAC	3,000		eGFR: 45 mL/min	I: both variables below the cutoffs II: 1 variable above the cutoff III: both variables above the cutoff
Expanded NAC	3,000 and 10,000		eGFR: 45 mL/min	I: both variables below the cutoffs II: 1 variable above the cutoff III: both variables above the cutoff IV: NT-proBNP >10,000 regardless of eGFR

AL = light chain; ATTR = transthyretin; BNP = B-type natriuretic peptide; dFLC = difference between involved and uninvolved serum free light chains; eGFR = estimated glomerular filtration rate; NAC = National Amyloidosis Centre; NT-proBNP = N-terminal pro-B-type natriuretic peptide.

promising role to play in the diagnosis and prognosis of CA, and the evidence is progressively accumulating.[56] It is possible that PET tracers will play a key role in early diagnosis and may even be sensitive enough to detect patients with cardiac amyloid deposits who have not yet undergone the structural and functional changes that result in cardiac amyloidosis. Larger multicenter studies are required to further assess their diagnostic performance relative to other established imaging modalities.

STRATIFYING PROGNOSIS

In the context of systemic amyloidosis, cardiac involvement is the main driver of morbidity and mortality; therefore, any measure of CA burden remains highly prognostic. The most widely used disease staging systems use common serum biomarkers. In patients with AL-CA, the Mayo classification used a combination of N-terminal pro-B-type natriuretic peptide (NT-proBNP) and troponin to stratify prognosis at the time of diagnosis and, more recently, the addition of differential FLC has been added to the classification.[57] Boston University also developed a staging system based on brain natriuretic peptide (BNP) and troponin, which has a high concordance with the Mayo staging system.[58]

The Mayo clinic has developed a risk stratification system for patients with wtATTR-CA that also uses NT-proBNP and troponin,[59] whereas the staging developed at the National Amyloidosis Centre (NAC), uses a combination of NT-proBNP and estimated glomerular filtration rate to stratify patients and is applicable for patients with wtATTR-CA and hereditary transthyretin CA.[7] Both staging systems used the same NT-proBNP cutoff of 3,000 ng/L, but the NAC staging system was recently expanded to include a 4th stage with an NT-proBNP cutoff of 10,000 ng/L which identifies patients at the highest risk of early mortality (**Table 1**).[60] Both staging systems have been improved by incorporating NYHA functional class and loop diuretic dose in what is known as the Columbia staging system,[61] and the risk of mortality can be further refined by assessing multiple additional commonly measured serum and urinary biomarkers.[62,63] NT-proBNP forms the cornerstone of all biomarker-based staging systems; however, elevations represent the final common pathway of several mechanisms integrating renal impairment, fluid status, neurohormonal activation,

and cardiac function rather than serving as a direct measure of the CA burden. Therefore, imaging-based metrics that more accurately reflect the magnitude of amyloid infiltration can refine prognostic stratification at diagnosis.

A wide array of structural and functional echocardiographic parameters are associated with an increased risk of mortality, with longitudinal strain remaining independently associated with mortality even after adjusting for the respective biomarker-based staging systems. The strong prognostic association of longitudinal strain is likely related to amyloid infiltration beginning at the endocardium, where longitudinal fibers are situated; therefore, measures of longitudinal systolic function reflect the whole spectrum of disease from early to advanced stages.[23,64] Stroke volume also represents an important prognostic marker. Typically, CA results in a low stroke volume, secondary to systolic impairment, concentric remodeling, and a small LV cavity. Therefore, indexed stroke volume represents a comprehensive measure of disease burden that reflects both structural and functional changes.[23,65] Myocardial contraction index is the ratio of stroke volume to myocardial volume and is a volumetric measure of myocardial shortening analogous to strain, which also represents an important prognostic marker that is superior to ejection fraction.[66]

Tissue characterization through use of advanced CMR techniques adds incremental information to the structural and functional parameters by providing a detailed description of the myocardial composition. Transmurality of LGE provides important prognostic information, with the presence of transmural LGE being independently associated with a 4-fold higher risk of mortality.[27] The development of ECV mapping as a direct measure of myocardial extracellular expansion in the presence of amyloid deposition represented a major step in directly quantifying amyloid load, with ECV remaining an independent predictor of prognosis.[67,68] Precontrast native T1 also represents a prognostic marker, but only ECV remains independently associated with mortality even after adjusting for biomarker stage, suggesting that it is a more robust marker of disease burden. These differences are likely due to different biological information being captured, with native T1 providing a composite signal from the intracellular and extracellular space, a signal that is potentially influenced by other pathophysiological mechanisms beyond simple amyloid deposition, whereas ECV acts as a direct measure of the amyloid burden.[68] In the context of systemic AL amyloidosis, hepatic ECV, as a marker of liver amyloid load, also remains independently associated with mortality after adjusting for the Mayo staging criteria, myocardial ECV, and splenic ECV.[30]

Although cardiac scintigraphy with bone-avid radiotracers represents a sensitive test to diagnose ATTR-CA, it remains unclear whether the degree of myocardial radiotracer uptake is able to accurately quantify amyloid burden and estimate prognosis. In patients with known ATTR-amyloidosis, the presence of any cardiac uptake (ie, Perugini grade >0) and a heart-to-contralateral ratio >1.6 confers a worse prognosis; however, in patients with established CA, there is no difference in survival between those with grade 2 or 3 cardiac uptake.[69,70] Further studies are needed to assess whether heart-to-whole-body ratio and quantitative standardized uptake value (SUV) measures are able to refine prognostic stratification in patients with established CA.

The prognostic importance of PET tracer uptake has been shown in patients with AL-CA, whereby increased myocardial uptake of PIB portends worse prognosis[71] and right ventricular uptake of ^{18}F-florbetapir was associated with an increased risk of major cardiovascular events.[51] However, PET tracers are investigational and not clinically approved for cardiac imaging. Larger multicenter studies are needed to assess whether amyloid burden estimated by cardiac PET adds incremental information to established staging systems.

DISEASE-MODIFYING THERAPIES FOR ATTR-CA

Until recently, the primary approach for managing patients with ATTR-CA was supportive therapy and use of loop diuretic agents to aid meticulous volume control. Two recent studies have shown that low-dose beta-blockers in patients with a reduced ejection fraction and both mineralocorticoid receptor antagonists and sodium-glucose co-transporter-2 inhibitors across the spectrum of disease were associated with improved survival. However, none of these medications specifically target the pathways responsible for ATTR amyloid fibril formation.[72,73] A deeper understanding of the underlying pathophysiology has resulted in the discovery of multiple different, disease specific pharmacotherapies that are either approved for clinical use or at different stages of development.[74-76] Considering the likely expansion of disease-modifying therapies, indicators of worsening disease might highlight the need to switch to alternative agents or consider combination therapy; however, at present, there is no consensus recommendation regarding how progression markers should guide treatment decisions. A large multicenter study recently showed that NT-proBNP progression

(defined as an increase >700 ng/L and >30%) and outpatient diuretic intensification represented markers of disease progression that were independently associated with a worse prognosis.[77] The change in 6-minute walk test can be leveraged as a marker of disease burden and an absolute reduction >35 m or relative reduction >5% is also associated with disease progression and independently associated with a worse prognosis (Table 2).[78] Serial echocardiographic assessments have shown that worsening of the degree of mitral and tricuspid regurgitation and a reduction in stroke volume are also associated with an increased risk of mortality.[24]

The search for various novel markers of disease progression and treatment response has expanded to the use of imaging-based assessments, with various different metrics being increasingly used in the context of clinical trials where imaging-based parameters are being leveraged as endpoints.[79]

TTR STABILIZERS. Current therapeutic strategies are aimed at reducing the formation of ATTR-amyloid fibrils. TTR stabilizers bind to the TTR tetramer and prevent dissociation into amyloidogenic monomers and oligomers that subsequently form pathogenic amyloid fibrils.[74]

DIFLUNISAL. Despite showing some efficacy in patients with ATTR-polyneuropathy (ATTR-PN), the experience of diflunisal in ATTR-CA is limited to small open-label studies, with 2 retrospective analyses suggesting an association with a reduced risk of mortality.[80,81]

Imaging-based studies suggest that diflunisal may slow disease progression. A prospective study has shown that 34 patients treated with diflunisal had a significant improvement in apical LV rotation/torsion[82] and a recent retrospective study of 81 patients confirmed that diflunisal stabilized global longitudinal strain (GLS), whereas GLS deteriorated in the untreated group.[83]

TAFAMIDIS. The ATTR-ACT (A Multicenter, International, Phase 3, Double-Blind, Placebo-Controlled, Randomized Study to Evaluate the Efficacy, Safety, and Tolerability of Daily Oral Dosing of Tafamidis Meglumine [PF-06291826] 20 mg or 80 mg in Comparison to Placebo in Subjects Diagnosed With Transthyretin Cardiomyopathy [TTR-CM]) trial showed that treatment with tafamidis reduced the hierarchical composite of all-cause mortality and cardiovascular hospitalisations.[74] Post hoc analysis of 436 patients with available echocardiographic data has shown that tafamidis was associated with a less pronounced worsening of stroke volume, GLS, and E/e′.[84] This was supported by a recent retrospective study of 45 patients (treated: 23, untreated: 22). Following 12-months of treatment, tafamidis was associated with an attenuated deterioration in GLS, myocardial work index, and efficiency.[17] A study of 40 patients treated with tafamidis who underwent serial bone scintigraphy scans demonstrated that treatment was associated with a significant reduction in SUV retention index, and patients with a greater reduction also experienced favorable biochemical and echocardiographic changes.[85]

TABLE 2 Measures of Disease Progression and Treatment Response in Cardiac Amyloidosis

Markers	Definition
Measures of disease progression in cardiac ATTR amyloidosis	
NT-proBNP	NT-proBNP progression defined as an increase of >700 ng/L and >30%
Loop diuretic dose	Outpatient diuretic intensification defined as any initiation or increment in the dose of loop diuretic
6-minute walk test distance	Absolute reduction defined as a decrease >35 m Relative reduction defined as a decrease >5%
KCCQ	Worsening of the KCCQ
Mitral regurgitation	Worsening of mitral regurgitation
Tricuspid regurgitation	Worsening of tricuspid regurgitation
Measures of treatment response in cardiac AL amyloidosis	
NT-proBNP	NT-proBNP response defined as a decrease of >300 ng/L and >30%
Longitudinal strain	Longitudinal strain response defined as an improvement ≥2%
Native T1	Reduction in native-T1 ≥50 ms
Extracellular volume	Reduction in extracellular volume ≥5%

KCCQ = Kansas City Cardiomyopathy Questionnaire; other abbreviations as in Table 1.

ACORAMIDIS. The ATTRibute-CM (A Phase 3, Randomized, Double-Blind, Placebo-Controlled Study of the Efficacy and Safety of AG10 in Subjects With Symptomatic Transthyretin Amyloid Cardiomyopathy) trial has shown that treatment was associated with a favorable win ratio in a 4-component hierarchical analysis that included all-cause mortality, cumulative frequency of cardiovascular-related hospitalization, change in NT-proBNP, and change in 6-minute walk test distance to assess the efficacy of acoramidis.[86] Serial CMR scans were also used in a small subset of patients to assess changes in CMR parameters in response to treatment. The study was limited by a small sample size but showed favorable trends in CMR parameters in the treatment group compared with placebo, and a small proportion of the treatment group demonstrated amyloid regression compared to none in the placebo group.[87]

GENE SILENCERS AND GENE EDITING THERAPIES. The circulating TTR amyloid precursor protein is

synthesized by the liver and coded for by a single gene, making ATTR-amyloidosis the prototypic model disease for targeted gene interference therapies.[75]

PATISIRAN. The APOLLO (A Phase 3 Multicenter, Multinational, Randomized, Double-blind, Placebo-controlled Study to Evaluate the Efficacy and Safety of Patisiran [ALN-TTR02] in Transthyretin [TTR]-Mediated Polyneuropathy [Familial Amyloidotic Polyneuropathy-FAP]) trial demonstrated efficacy of patisiran in patients with ATTR-PN. A post hoc analysis on a subset of 126 patients considered to have cardiac involvement (defined as LV wall thickness >13 mm in the absence of known hypertension or significant aortic valve disease) demonstrated that patisiran was associated with a reduced mean LV wall thickness and relative wall thickness, and improved GLS compared with placebo. However, the definition of cardiac involvement is nonspecific and could have resulted in the inclusion of patients who do not fulfil the guideline-mandated diagnostic criteria for ATTR-CA.[88]

Following this, the APOLLO-B (A Phase 3, Randomized, Double-blind, Placebo-controlled Multicenter Study to Evaluate the Efficacy and Safety of Patisiran in Patients With Transthyretin Amyloidosis With Cardiomyopathy [ATTR Amyloidosis With Cardiomyopathy]) trial demonstrated that treatment with patisiran resulted in a slower decline in 6-minute walk test distance (mean difference: 14.7 m).[89] However, the U.S. Food and Drug Administration declined the application to approve patisiran for the treatment of ATTR-CA, expressing concerns that the small effect size was not clinically meaningful. Although patients who were initially in the placebo group showed stabilization of their functional capacity during the open label extension, the decline that occurred in the first 12 months was not recoverable. This observation emphasizes the importance of initiating treatment early in the disease process.[90]

A small imaging-based study of 16 patients yielded results that support the efficacy of patisiran in treatment of ATTR-CA, with treatment being associated with a reduction in NT-proBNP, ECV, and a reduction in myocardial radiotracer uptake on bone scintigraphy in a proportion of patients. Although the reduction in cardiac uptake showed a favorable effect of patisiran, the kinetics and dynamics of radiotracers binding to the myocardium, bones, and soft tissues may fluctuate; therefore, variations in any of these organs will influence both the visual appearance and mathematical calculation of proportionate myocardial radiotracer uptake. Therefore, reduced myocardial uptake should always be supported by improvements in other measures of cardiac function before the observed changes are ascribed exclusively to a reduction in CA burden.[42] Larger-scale imaging-based studies are required to confirm whether treatment with patisiran is able to impact the amyloid load, while an assessment of more conventional endpoints such as mortality and cardiovascular hospitalizations may offer additional clarification into efficacy.[91]

VUTRISIRAN. Vutrisiran demonstrated efficacy in patients with ATTR-PN in the HELIOS-A (A Phase 3 Global, Randomized, Open-label Study to Evaluate the Efficacy and Safety of ALN-TTRSC02 in Patients With Hereditary Transthyretin Amyloidosis) trial. A post hoc analysis assessed the impact of vutrisiran on cardiac parameters. In the overall study population, and in those considered to have cardiac involvement (based on the prespecified definition used in the post hoc APOLLO analysis), treatment with vutrisiran was associated with beneficial changes in NT-proBNP and a nominally significant beneficial change in stroke volume compared with placebo. This study used a historical placebo group from the APOLLO trial, and there were significant differences in baseline characteristics between the treatment and placebo groups. Furthermore, the definition of cardiac involvement is nonspecific and fraught with the same limitations as the post hoc analysis of the APOLLO trial.[43]

The HELIOS-B (A Phase 3, Randomized, Double-blind, Placebo-controlled, Multicenter Study to Evaluate the Efficacy and Safety of Vutrisiran in Patients With Transthyretin Amyloidosis With Cardiomyopathy) trial showed that treatment with vutrisiran was associated with a reduction in the composite of all-cause mortality and recurrent cardiovascular events in the overall population and monotherapy population (who were not treated with tafamidis at enrolment).[92]

EPLONTERSEN. Eplontersen has shown efficacy in patients with ATTR-PN in the NEURO-TTRansform (A Phase 3 Global, Open-Label, Randomized Study to Evaluate the Efficacy and Safety of ION-682884 in Patients With Hereditary Transthyretin-Mediated Amyloid Polyneuropathy) trial.[93] A post hoc analysis of the change in echocardiographic parameters in patients treated with eplontersen compared to the historical placebo group from NEURO-TTR showed that, in the overall population, eplontersen was associated with improvements in LV end-diastolic volume, stroke volume, E/e′, and left atrial volume. In a subgroup of patients considered to have cardiac involvement (based on the prespecified definition

used in the post hoc APOLLO analysis), treatment with eplontersen was associated with an improvement in LV stroke volume and ejection fraction. However, due to the study design and use of a historical cohort from the NEURO-TTR (A Phase 2/3 Randomized, Double-Blind, Placebo-Controlled Study to Assess the Efficacy and Safety of ISIS 420915 in Patients With Familial Amyloid Polyneuropathy) trial, this study is burdened with the same limitations as the post hoc analyses of the APOLLO and HELIOS-A trial populations.[94]

The CARDIO-TTRansform (A Phase 3 Global, Double-Blind, Randomized, Placebo-Controlled Study to Evaluate the Efficacy and Safety of ION-682884 in Patients With Transthyretin-Mediated Amyloid Cardiomyopathy) trial is designed to assess the efficacy of eplontersen in ATTR-CA and will assess a primary endpoint of a composite of cardiovascular mortality and recurrent cardiovascular events. This trial has recruited more than 1,400 patients, many of whom are also being treated with tafamidis. Considering the large study population, CARDIO-TTRansform (NCT04136171) is well placed to assess the efficacy of combination therapy. Serial CMR scans are also used in a large subset of patients to assess changes in parameters in response to treatment, with ECV being used as a surrogate measure of the CA burden.

NTLA-2001. NTLA-2001 harnesses CRISPR-Cas9 technology to permanently edit the TTR gene. NTLA-2001 was tested in a small cohort of patients with ATTR-amyloidosis and was tolerated without any serious adverse events.[95] A phase 3 trial has been designed to assess the efficacy of NTLA-2001 in ATTR-CA and will assess a primary endpoint of a composite of cardiovascular mortality and cardiovascular events. The MAGNITUDE trial (NCT06128629) will use serial CMR scans in a large group of patients to assess changes in cardiac structure, function, and ECV in response to treatment.

ANTIAMYLOID THERAPIES. TTR stabilizers and gene-modulating therapies all reduce the formation of amyloid fibrils but do not accelerate removal of fibrils that have accumulated in the myocardium. Amyloid removal represents a significant unmet clinical need, especially for patients diagnosed with advanced cardiac disease. Antibody-mediated amyloid removal was recently depicted in 3 patients who spontaneously developed antibodies to ATTR-amyloid, which was associated with reversion to near-normal cardiac structure and function. CMR confirmed regression of LGE burden and ECV. This exciting discovery provided proof of concept that antibody-based therapies can facilitate amyloid removal and result in subsequent disease reversal.[96]

There are several investigational antiamyloid therapies at various stages of development, of which NI006 (also known as ALXN2220) is at the most advanced stage. A phase 1 trial of 40 patients with ATTR-CA demonstrated that NI006 was safe and at higher doses appeared to induce disease regression with reductions in serum biomarkers and myocardial ECV.[97]

PRX004 (coramitug) has been evaluated in a phase 1 dose escalation study in 21 patients with either ATTR-CA or ATTR-PN and has shown that PRX004 was safe and in all 7 evaluable patients; there was an improvement in echocardiographic GLS. Although these results have been presented, the full results have yet to be published.[98]

AT-02 binds all forms of amyloid with a high affinity, and the immunoglobulin promotes macrophage-mediated phagocytosis of amyloid fibrils.[99] A phase 1 study, A Study of AT-02 in Subjects With Systemic Amyloidosis (NCT05951049), which will assess the safety of AT-02 and efficacy using serial CMR scans with ECV mapping in patients with various forms of amyloidosis, is currently ongoing (**Table 3**).

TRACKING TREATMENT RESPONSE IN AL-CA

Cytotoxic chemotherapy aimed at suppressing light-chain production forms the mainstay of treatment for AL-CA. A deep and rapid reduction in the amyloid precursor protein prevents further formation of amyloid fibrils and halts disease progression. A 2-pronged approach is used to assess treatment response and is comprised of measuring the reduction in FLCs and the direct impact of treatment on the heart. Changes in NT-proBNP have been widely used to assess the cardiac treatment response but, as noted, also reflect multiple extracardiac variables.[100] More recently, multimodality cardiac imaging has emerged as an important adjunct that represents a noninvasive measure of the changes in amyloid burden in response to treatment. Novel therapies are being developed to target the amyloid fibrils that have already accumulated within the myocardium, such as anselamimab and birtamimab (antibodies targeted at light-chain amyloid deposits).[101,102] The role of cardiac imaging is likely to expand in the near future, with the ability to measure changes in the CA burden being of great importance in evaluating the efficacy of these new agents.

TABLE 3 ATTR Specific Disease Modifying Therapies

Drug	Mechanism of Action	Stage of Approval	Route of Administration	Dose	Phase 3 Clinical Trial	Cardiovascular Trial Outcomes	Side Effects
Transthyretin stabilizers							
Diflunisal	Stabilizes TTR to prevent dissociation	Approved as an NSAID, off-license use for ATTR-CA and ATTR-PN	Oral	250 mg twice daily	NA	Small retrospective studies have demonstrated an association with reduced mortality	Fluid retention Bleeding Renal dysfunction
Tafamidis	Stabilizes TTR to prevent dissociation	Approved for ATTR-CA and ATTR-PN	Oral	Vyndamax 61 mg or Vyndaquel 80 mg once daily	ATTR-ACT	RCT demonstrating a reduction in the hierarchical composite of all-cause mortality and cardiovascular hospitalizations, along with reduced rates of 6MWT and KCCQ decline	None
Acoramidis	Stabilizes TTR to prevent dissociation	Due to be reviewed by the FDA	Oral	800 mg twice daily	ATTRibute-CM	RCT demonstrating a reduction in the hierarchical composite of all-cause mortality, cardiovascular hospitalizations, change in NT-proBNP, and change in 6MWT, along with reduced rates of 6MWT distance and KCCQ decline	None
Gene silencers							
Patisiran	siRNA targeting TTR mRNA	Approved for ATTR-PN, but not for ATTR-CA	Intravenous infusion	80-min infusion based on body weight every 3 wks: <100 kg = 0.3 mg/kg; >100 kg = 30 mg	APOLLO-B	RCT demonstrating a reduction in the rate of 6MWT distance decline compared with placebo, along with a reduced rate of KCCQ decline	Infusion related reactions Vitamin A deficiency Peripheral oedema
Vutrisiran	siRNA targeting TTR mRNA	Approved for ATTR-PN, but not for ATTR-CA	Subcutaneous injection	25 mg injection every 3 months	HELIOS-B	RCT demonstrating a reduction in the composite of all-cause mortality and recurrent cardiovascular events in the overall population and the monotherapy population, along with reduced rates of 6MWT distance and KCCQ decline	Infusion related reactions Vitamin A deficiency Nasopharyngitis Headache Urinary tract infections Dyslipidemia
Eplontersen	ASO inhibitor of TTR production	Approved for ATTR-PN, but not for ATTR-CA	Subcutaneous injection	45 mg monthly	CARDIO-TTRansform	CARDIO-TTRansform is a phase 3 RCT designed to assess the efficacy of eplontersen in patients with ATTR-CA	Headache Vitamin A deficiency

Continued on the next page

A small retrospective study has shown that patients who achieved a complete hematological response displayed improvements in longitudinal strain alongside reductions in NT-proBNP and troponin-I.[103] These observations were supported by a larger prospective study confirming that patients who achieved a complete hematological response experienced an improvement in longitudinal strain, and a clinically significant improvement in longitudinal strain (≥2%) was independently associated with a reduced risk of mortality.[64] Following these results, change in GLS has been used as an exploratory endpoint in a phase 2 trial of anselamimab, whereby treatment resulted in a significant improvement in GLS in 9 of 10 patients.[101]

Advances in CMR techniques have enabled the assessment of changes in the myocardial tissue composition in response to treatment, with global changes in ECV representing an accurate surrogate marker of the change in CA burden. A prospective study of patients with AL-CA treated with first-line bortezomib-based chemotherapy has shown that

TABLE 3 Continued

Drug	Mechanism of Action	Stage of Approval	Route of Administration	Dose	Phase 3 Clinical Trial	Cardiovascular Trial Outcomes	Side Effects
Gene editing therapy							
NTLA-2001	CRISP-Cas9 editing of the TTR gene	Under investigation	Intravenous infusion	0.1 mg/kg or 0.3 mg/kg given once	NA	A small phase 1 trial has demonstrated that NTLA-2001 is safe and results in a sustained TTR knockdown	Headache Vitamin A deficiency
Anti-ATTR amyloid therapies							
NI006	Recombinant human anti-ATTR monoclonal IgG1 antibody that binds ATTR-amyloid	Under investigation	Intravenous infusion	4 weekly infusions with doses ranging from 0.3-60 mg/kg	NA	A small phase 1 trial has demonstrated that NI006 is safe and at higher doses appeared to reduce NT-proBNP, troponin I, and myocardial extracellular volume. A phase 3 trial will assess efficacy in ATTR-CA.	Arthralgia Thrombocytopenia
PX004	Humanized IgG antibody that binds ATTR-amyloid	Under investigation	Intravenous infusion	4 weekly infusions with doses ranging from 0.1-3.0 mg/kg	NA	A small phase 1 trial has demonstrated that PX004 is safe	Unknown
AT-02	Pan amyloid removal technology using a single-chain fusion protein to stimulate immunological removal of amyloid	Under investigation	Intravenous infusion	Dosing not available	NA	A small phase 1 trial is currently ongoing	Unknown

6MWT = 6-minute walk test; ASO = antisense oligonucleotide; CA = cardiac amyloidosis; FDA = U.S. Food and Drug Administration; IgG = immunoglobulin G; mRNA = messenger RNA; NA = not available; NSAID = nonsteroidal anti-inflammatory drug; PN = polyneuropathy; RCT = randomized controlled trial; siRNA = small interfering RNA; TTR = transthyretin; other abbreviations as in Tables 1 and 2.

some patients who achieved a deep and rapid hematological response attained myocardial ECV regression which occurred before any detectible changes in cardiac structure and function. However, not all patients with a deep reduction in the amyloid precursor protein attained disease regression, suggesting that this is not sufficient alone. Amyloid deposition involves constant turnover with disease progression occurring when the rate of formation exceeds clearance, and regression vice versa. Therefore, regression is equally dependent on a deep hematological response and intrinsic amyloid clearance mechanisms. Multiparametric mapping has enhanced our understanding of cardiac response to treatment, with reductions in ECV being followed by improvements in systolic function and reductions in LV mass. Changes in ECV remained independently associated with prognosis, even after adjusting for the hematological, NT-proBNP, and longitudinal strain response (Figure 7).[104]

Multiorgan ECV measurements have also shown utility in tracking the hepatic and splenic response to treatment. The changes in visceral organ ECV correlate well with changes in amyloid burden measured by SAP scintigraphy and serum biomarkers reflective of the organ amyloid load. The rate of regression varied between organs with the visceral organs demonstrating a faster rate of regression than the heart, suggesting different rates of amyloid clearance in different organs. Changes in hepatic and splenic ECV were associated with prognosis, with the change in hepatic ECV remaining independently associated with mortality after adjusting for the hematological response, NT-proBNP response, and change in myocardial and splenic ECV. The absence of ionizing radiation and the excellent safety profile of gadolinium-based contrast agents allow for the safe integration of serial CMR scans into clinical practice to track the multiorgan treatment response.[30]

Serial myocardial native-T1 measurements are also able to track the cardiac treatment response, with reductions in native T1 being associated with favorable biochemical, structural, and functional changes. Native T1 represents a composite signal influenced by intracellular and extracellular space. Therefore, changes in native T1 reflected both changes in the

FIGURE 7 **Changes on CMR Imaging in Response to Treatment in the Context of Cardiac Light Chain Amyloidosis**

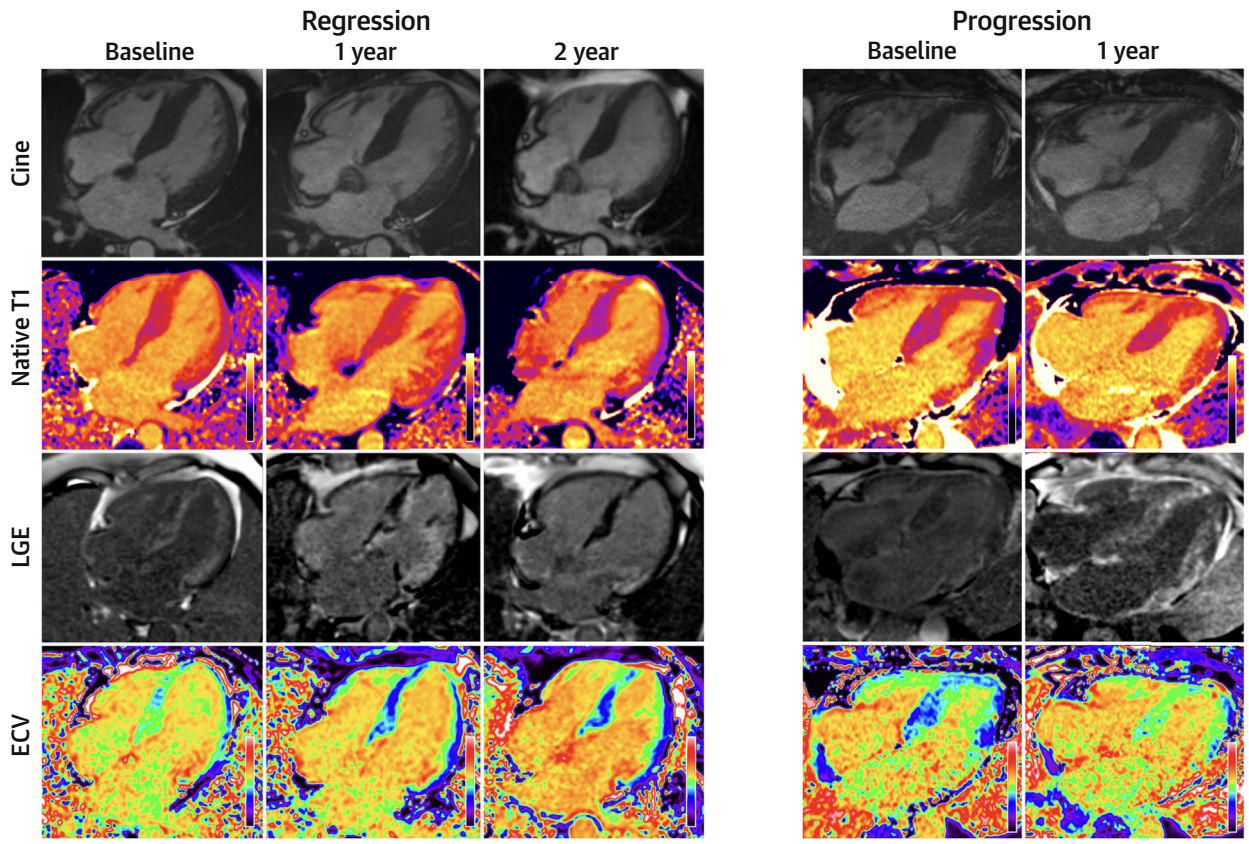

Abbreviations as in Figure 3.

amyloid burden and myocardial edema, and importantly remained independently associated with prognosis.[105]

Early investigational data suggest that changes in PET tracer uptake may be used to track the treatment response, with one small study showing that patients deemed to have active AL-CA had a higher ^{18}F-florbetapir cardiac uptake than those in remission.[51] However, this study lacked serial imaging with longitudinal follow-up; therefore, further studies are needed to investigate whether these changes not only correlate with changes in established markers of disease burden but also prognosis.

FUTURE PERSPECTIVES

CA has become an increasingly recognized cause of heart failure, and increased awareness together with advanced diagnostics and the emergence of disease specific therapies have all contributed to patients being diagnosed earlier in the disease course. However, a significant proportion of patients are still diagnosed with advanced cardiac disease. The development of screening programs may offer an opportunity to detect patients at an earlier disease stage. A focus on developing automated screening algorithms that could flag a suspicion of CA from a routine echocardiogram could result in more patients being detected at earlier disease stages and facilitate the prompt initiation of disease modifying therapies.

Artificial intelligence may not only improve diagnostic accuracy but also the elimination of manual operator contouring and it provides highly reproducible and precise measurements, which is fundamental when tracking changes in response to treatment, especially when changes over time in these parameters are considered minimal.[24,79] The ability to track the change in amyloid burden in response to treatment is of increasing importance especially considering the impending availability of

CENTRAL ILLUSTRATION **Typical Imaging Features for a Patient With Cardiac Transthyretin Amyloidosis**

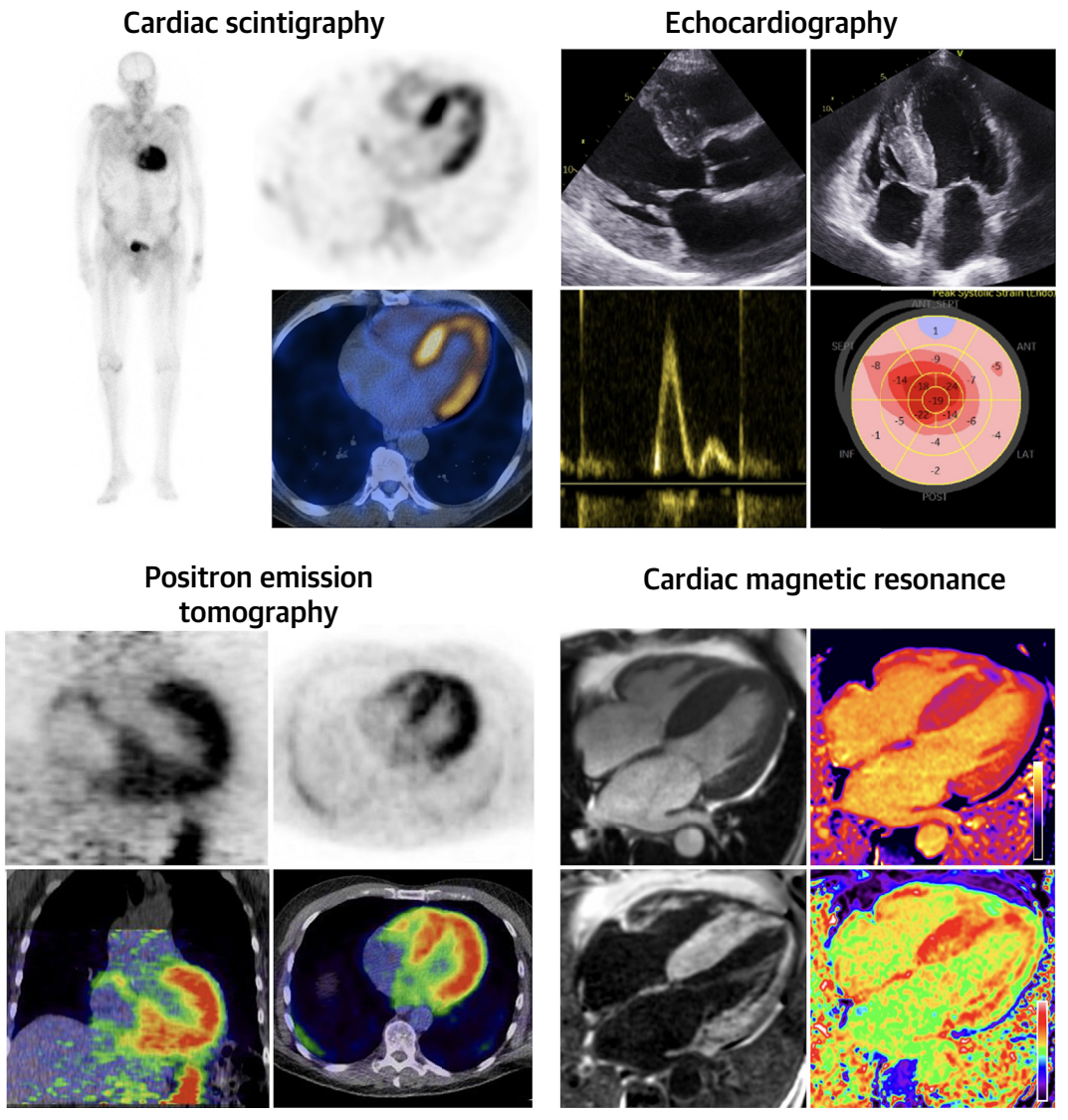

Fontana M, et al. JACC Cardiovasc Imaging. 2025;18(4):478-499.

multiple disease modifying therapeutic options as well as the development of several compounds that promote regression by directly targeting and enhancing the clearance of existing amyloid deposits. CMR with multiparametric mapping has already demonstrated utility in tracking changes in the amyloid burden and, although PET and other tracers remain at an early investigational stage, preliminary data suggest that serial studies may also be able to track changes in response to treatment. Multimodality imaging studies are required to further optimize the precision of each imaging modality and decipher which modality is most suited to tracking changes over time.

CONCLUSIONS

Advances in cardiac imaging techniques have transformed the ability to diagnose, prognosticate, and treat patients with CA (Central Illustration). The additional information obtained from advanced cardiac imaging, such as multiparametric mapping, has

HIGHLIGHTS

- Cardiac amyloidosis represents an infiltrative cardiomyopathy characterized by accumulation of amyloid fibrils within the myocardium.
- Advances in multimodality imaging have facilitated earlier diagnosis and prompt initiation of disease modifying therapies.
- Cardiac imaging will play a key role in tracking treatment response.
- Research focused on improved precision may augment detection of changes earlier during treatment.

enhanced our understanding of the underlying disease process and identified noninvasive measures of the CA burden, which enable direct visualization of the impact of disease modifying therapies, with successful treatments resulting in amyloid removal and disease regression. Cardiac imaging has enabled clinicians to understand how the myocardium responds to treatment and allowed clinicians to tailor treatment strategies to each individual patient. As technology advances, the integration of artificial intelligence represents the next frontier, and the application of automated algorithms to large data sets may enable further improvements in diagnostic accuracy, potentially resulting in earlier diagnosis and improvements in precision that are likely to enhance our ability to track the change in CA burden in response to treatment.

FUNDING SUPPORT AND AUTHOR DISCLOSURES

Dr Fontana has received support from the British Heart Foundation Intermediate Clinical Research Fellowship (FS/18/21/33447) and has received consulting fees from Intellia, Novo-Nordisk, Pfizer, Eidos, Prothena, Akcea, Alnylam, Caleum, Alexion, Janssen, Ionis, and AstraZeneca. Dr Cuddy has received grants from National Institutes of Health award National Institutes of Health 1K23HL166686-01 and the American Heart Association award 23CDA857664; and has served on advisory boards for Bridge Bio, Ionis, Alexion Pharmaceuticals, AstraZeneca, and Novo Nordisk. Dr Singh has received grants from the American Society of Nuclear Cardiology/Pfizer and is on the speakers bureau for Pfizer and AstraZeneca. Dr Hanna has served on advisory boards for Alnylam, Bridge Bio, Pfizer, Ionis, and Alexion Pharmaceuticals. Dr Ruberg has received grants from National Institutes of Health awards R01HL139671 and R01AG081582; has received research grants to his institution from Akcea, Anumana, and Pfizer; and has received consulting fees from AstraZeneca and Attralus. Dr Grogan has received grants and/or consulting fees paid to her institution from Anumana, Alnylam, AstraZeneca, Attralus, BridgeBio/Eidos, Pfizer, Janssen, and NovoNordisk. Dr Gilmore has received consulting fees from Ionis, Eidos, Intellia, Alnylam, and Pfizer.

ADDRESS FOR CORRESPONDENCE: Dr Marianna Fontana, National Amyloidosis Centre, University College London, Royal Free Hospital, Rowland Hill Street, London NW3 2PF, United Kingdom. E-mail: m.fontana@ucl.ac.uk.

REFERENCES

1. Wechalekar AD, Gillmore JD, Hawkins PN. Systemic amyloidosis. *Lancet*. 2016;387:2641–2654.

2. Ruberg FL, Grogan M, Hanna M, Kelly JW, Maurer MS. Transthyretin amyloid cardiomyopathy: JACC State-of-the-Art Review. *J Am Coll Cardiol*. 2019;73:2872.

3. Falk RH, Alexander KM, Liao R, Dorbala S. AL (light-chain) cardiac amyloidosis: a review of diagnosis and therapy. *J Am Coll Cardiol*. 2016;68:1323–1341.

4. Ioannou A, Porcari A, Patel RK, et al. Rare forms of cardiac amyloidosis: diagnostic clues and phenotype in Apo AI and AIV amyloidosis. *Circ Cardiovasc Imaging*. 2023;16:523–535.

5. Patel RK, Ioannou A, Razvi Y, et al. Sex differences among patients with transthyretin amyloid cardiomyopathy—from diagnosis to prognosis. *Eur J Heart Fail*. 2022;24:2355–2363.

6. Porcari A, Razvi Y, Masi A, et al. Prevalence, characteristics and outcomes of older patients with hereditary versus wild-type transthyretin amyloid cardiomyopathy. *Eur J Heart Fail*. 2023;25:515–524.

7. Gillmore JD, Damy T, Fontana M, et al. A new staging system for cardiac transthyretin amyloidosis. *Eur Heart J*. 2018;39:2799–2806.

8. Ioannou A, Patel RK, Razvi Y, et al. Impact of earlier diagnosis in cardiac ATTR amyloidosis over the course of 20 years. *Circulation*. 2022;146:1657–1670.

9. González-López E, Gallego-Delgado M, Guzzo-Merello G, et al. Wild-type transthyretin amyloidosis as a cause of heart failure with preserved ejection fraction. *Eur Heart J*. 2015;36:2585–2594.

10. Castano A, Narotsky DL, Hamid N, et al. Unveiling transthyretin cardiac amyloidosis and its predictors among elderly patients with severe aortic stenosis undergoing transcatheter aortic valve replacement. *Eur Heart J*. 2017;38:2879–2887.

11. Abouezzeddine OF, Davies DR, Scott CG, et al. Prevalence of transthyretin amyloid cardiomyopathy in heart failure with preserved ejection fraction. *JAMA Cardiol*. 2021;6:1267–1274.

12. Knight DS, Zumbo G, Barcella W, et al. Cardiac structural and functional consequences of amyloid deposition by cardiac magnetic resonance and echocardiography and their prognostic roles. *JACC Cardiovasc Imaging*. 2019;12:823–833.

13. Liu D, Hu K, Niemann M, et al. Effect of combined systolic and diastolic functional parameter assessment for differentiation of cardiac amyloidosis from other causes of concentric left ventricular hypertrophy. *Circ Cardiovasc Imaging*. 2013;6:1066–1072.

14. Singh V, Soman P, Malhotra S. Reduced diagnostic accuracy of apical-sparing strain abnormality for cardiac amyloidosis in patients with chronic kidney disease. *J Am Soc Echocardiogr*. 2020;33:913–916.

15. Cuddy SAM, Datar Y, Ovsak G, et al. Optimal echocardiographic parameters to improve the diagnostic yield of Tc-99m-bone avid tracer cardiac scintigraphy for transthyretin cardiac amyloidosis. *Circ Cardiovasc Imaging*. 2022;15:E014645.

16. Boldrini M, Cappelli F, Chacko L, et al. Multiparametric echocardiography scores for the diagnosis of cardiac amyloidosis. *JACC Cardiovasc Imaging*. 2020;13:909–920.

17. Giblin GT, Cuddy SAM, González-López E, et al. Effect of tafamidis on global longitudinal strain and myocardial work in transthyretin cardiac amyloidosis. *Eur Heart J Cardiovasc Imaging*. 2022;23:1029.

18. Phelan D, Collier P, Thavendiranathan P, et al. Relative apical sparing of longitudinal strain using two-dimensional speckle-tracking echocardiography is both sensitive and specific for the diagnosis of cardiac amyloidosis. *Heart*. 2012;98:1442–1448.

19. Cotella J, Randazzo M, Maurer MS, et al. Limitations of apical sparing pattern in cardiac amyloidosis: a multicentre echocardiographic study. *Eur Heart J Cardiovasc Imaging*. 2024;25:754–761.

20. Goto S, Mahara K, Beussink-Nelson L, et al. Artificial intelligence-enabled fully automated detection of cardiac amyloidosis using electrocardiograms and echocardiograms. *Nat Comm*. 2021;12:1–12.

21. Bandera F, Martone R, Chacko L, et al. Clinical importance of left atrial infiltration in cardiac transthyretin amyloidosis. *JACC Cardiovasc Imaging*. 2021;15:17–29.

22. Martinez-Naharro A, Gonzalez-Lopez E, Corovic A, et al. High prevalence of intracardiac thrombi in cardiac amyloidosis. *J Am Coll Cardiol*. 2019;73:1733–1734.

23. Chacko L, Martone R, Bandera F, et al. Echocardiographic phenotype and prognosis in transthyretin cardiac amyloidosis. *Eur Heart J*. 2020;41:1439–1447.

24. Chacko L, Karia N, Venneri L, et al. Progression of echocardiographic parameters and prognosis in transthyretin cardiac amyloidosis. *Eur J Heart Fail*. 2022;24:1700–1712.

25. Ioannou A, Patel RK, Razvi Y, et al. Multi-imaging characterization of cardiac phenotype in different types of amyloidosis. *JACC Cardiovasc Imaging*. 2022;14:464–477.

26. Hawkins PN, Lavender JP, Pepys MB. Evaluation of systemic amyloidosis by scintigraphy with 123I-labeled serum amyloid P component. *N Engl J Med*. 1990;323:508–513.

27. Fontana M, Pica S, Reant P, et al. Prognostic value of late gadolinium enhancement cardiovascular magnetic resonance in cardiac amyloidosis. *Circulation*. 2015;132:1570–1579.

28. Fontana M, Banypersad SM, Treibel TA, et al. Native T1 mapping in transthyretin amyloidosis. *JACC Cardiovasc Imaging*. 2014;7:157–165.

29. Fontana M, Banypersad SM, Treibel TA, et al. Differential myocyte responses in patients with cardiac transthyretin amyloidosis and light-chain amyloidosis: a cardiac MR imaging study. *Radiology*. 2015;277:388–397.

30. Ioannou A, Patel RK, Martinez-Naharro A, et al. Tracking multiorgan treatment response in systemic AL-amyloidosis with cardiac magnetic resonance derived extracellular volume mapping. *JACC Cardiovasc Imaging*. 2023;16:1038–1052.

31. Kotecha T, Martinez-Naharro A, Treibel TA, et al. Myocardial edema and prognosis in amyloidosis. *J Am Coll Cardiol*. 2018;71:2919–2931.

32. Chacko L, Kotecha T, Ioannou A, et al. Myocardial perfusion in cardiac amyloidosis. *Eur J Heart Fail*. 2024;26:589–609.

33. Perugini E, Guidalotti PL, Salvi F, et al. Noninvasive etiologic diagnosis of cardiac amyloidosis using ^{99m}Tc-3,3-diphosphono-1,2-propanodicarboxylic acid scintigraphy. *J Am Coll Cardiol*. 2005;46:1076–1084.

34. Hanna M, Ruberg FL, Maurer MS, et al. Cardiac scintigraphy with technetium-99m-labeled bone-seeking tracers for suspected amyloidosis: JACC Review Topic of the Week. *J Am Coll Cardiol*. 2020;75:2851–2862.

35. Quarta CC, Zheng J, Hutt D, et al. ^{99m}Tc-DPD scintigraphy in immunoglobulin light chain (AL) cardiac amyloidosis. *Eur Heart J Cardiovasc Imaging*. 2021;22:1304–1311.

36. Gillmore JD, Maurer MS, Falk RH, et al. Nonbiopsy diagnosis of cardiac transthyretin amyloidosis. *Circulation*. 2016;133:2404–2412.

37. Rauf MU, Hawkins PN, Cappelli F, et al. Tc-99m labelled bone scintigraphy in suspected cardiac amyloidosis. *Eur Heart J*. 2023;24:2187–2198.

38. Dorbala S, Ando Y, Bokhari S, et al. ASNC/AHA/ASE/EANM/HFSA/ISA/SCMR/SNMMI expert consensus recommendations for multimodality imaging in cardiac amyloidosis: part 1 of 2—evidence base and standardized methods of imaging. *J Nucl Cardiol*. 2019;26:2065–2123.

39. Asif T, Gupta A, Murthi M, Soman P, Singh V, Malhotra S. Echocardiographic indices of left ventricular function and filling pressure are not related to blood pool activity on pyrophosphate scintigraphy. *J Nucl Cardiol*. 2023;30:708–715.

40. Singh V, Cuddy S, Kijewski MF, et al. Interobserver reproducibility and intra-observer repeatability in ^{99m}Tc-pyrophosphate scan interpretation for diagnosis of transthyretin cardiac amyloidosis. *J Nucl Cardiol*. 2022;29:440–446.

41. Castaño A, DeLuca A, Weinberg R, et al. Serial scanning with technetium pyrophosphate (^{99m}Tc-PYP) in advanced ATTR cardiac amyloidosis. *J Nucl Cardiol*. 2016;23:1355.

42. Fontana M, Martinez-Naharro A, Chacko L, et al. Reduction in CMR derived extracellular volume with patisiran indicates cardiac amyloid regression. *JACC Cardiovasc Imaging*. 2021;14:189–199.

43. Garcia-Pavia P, Grogan M, Kale P, et al. Impact of vutrisiran on exploratory cardiac parameters in hereditary transthyretin-mediated amyloidosis with polyneuropathy. *Eur J Heart Fail*. 2024;26:397–410.

44. Ross JC, Hutt DF, Burniston M, et al. Quantitation of ^{99m}Tc-DPD uptake in patients with transthyretin-related cardiac amyloidosis. *Amyloid*. 2018;25:203–210.

45. Antoni G, Lubberink M, Estrada S, et al. In vivo visualization of amyloid deposits in the heart with ^{11}C-PIB and PET. *J Nucl Med*. 2013;54:213–220.

46. Lee SP, Lee ES, Choi H, et al. ^{11}C-Pittsburgh B PET imaging in cardiac amyloidosis. *JACC Cardiovasc Imaging*. 2015;8:50–59.

47. Dorbala S, Cuddy S, Falk RH. How to image cardiac amyloidosis: a practical approach. *Cardiovasc Imaging*. 2020;13:1368–1383.

48. Park MA, Padera RF, Belanger A, et al. ^{18}F-Florbetapir binds specifically to myocardial light chain and transthyretin amyloid deposits. *Circ Cardiovasc Imaging*. 2015;8(8). https://doi.org/10.1161/CIRCIMAGING.114.002954

49. Dorbala S, Vangala D, Semer J, et al. Imaging cardiac amyloidosis: a pilot study using ^{18}F-florbetapir positron emission tomography. *Eur J Nucl Med Mol Imaging*. 2014;41:1652–1662.

50. Genovesi D, Vergaro G, Giorgetti A, et al. [^{18}F]-Florbetaben PET/CT for differential diagnosis among cardiac immunoglobulin light chain, transthyretin amyloidosis, and mimicking conditions. *JACC Cardiovasc Imaging*. 2021;14:246–255.

51. Cuddy SAM, Bravo PE, Falk RH, et al. Improved quantification of cardiac amyloid burden in systemic light chain amyloidosis: redefining early disease? *JACC Cardiovasc Imaging*. 2020;13:1325–1336.

52. Datar Y, Clerc OF, Cuddy SAM, et al. Quantification of right ventricular amyloid burden with ^{18}F-florbetapir positron emission tomography/computed tomography and its association with right ventricular dysfunction and outcomes in light-chain amyloidosis. *Eur Heart J Cardiovasc Imaging*. 2024;30:687–697.

53. Ehman EC, Samir El-Sady M, Kijewski MF, et al. Early detection of multiorgan light-chain amyloidosis by whole-body ^{18}F-florbetapir PET/CT. *J Nucl Med*. 2019;60:1234–1239.

54. Clerc OF, Cuddy SAM, Robertson M, et al. Cardiac amyloid quantification using ^{124}I-evuzamitide (^{124}I-P5+14) versus ^{18}F-florbetapir: a pilot PET/CT study. *Cardiovasc Imaging*. 2023;16:1419–1432.

55. Wall JS, Martin EB, Lands R, et al. Cardiac amyloid detection by PET/CT imaging of iodine (^{124}I) evuzamitide (^{124}I-p5+14): a phase 1/2 study. *JACC Cardiovasc Imaging*. 2023;16:1433–1448.

56. Singh V, Dorbala S. Positron emission tomography for cardiac amyloidosis: timing matters. *J Nucl Cardiol*. 2022;29:790–797.

57. Kumar S, Dispenzieri A, Lacy MQ, et al. Revised prognostic staging system for light chain amyloidosis incorporating cardiac biomarkers and serum free light chain measurements. *J Clin Oncol*. 2012;30:989.

58. Lilleness B, Ruberg FL, Mussinelli R, Doros G, Sanchorawala V. Development and validation of a survival staging system incorporating BNP in patients with light chain amyloidosis. *Blood*. 2019;133:215–223.

59. Grogan M, Scott CG, Kyle RA, et al. Natural history of wild-type transthyretin cardiac amyloidosis and risk stratification using a novel staging system. *J Am Coll Cardiol*. 2016;68:1014–1020.

60. Nitsche C, Ioannou A, Patel RK, et al. Expansion of the National Amyloidosis Centre staging system to detect early mortality in transthyretin cardiac amyloidosis. *Eur J Heart Fail*. 2024;26(9):2008–2012. https://doi.org/10.1002/ejhf.3354

61. Cheng RK, Levy WC, Vasbinder A, et al. Diuretic dose and NYHA functional class are independent predictors of mortality in patients with transthyretin cardiac amyloidosis. *JACC CardioOncol*. 2020;2:414–424.

62. Ioannou A, Nitsche C, Porcari A, et al. Multiorgan dysfunction and associated prognosis in transthyretin cardiac amyloidosis. *J Am Heart Assoc*. 2024;13:e033094.

63. Ioannou A, Rauf MU, Patel RK, et al. Albuminuria in transthyretin cardiac amyloidosis: prevalence, progression and prognostic importance. *Eur J Heart Fail*. 2024;26:65–73.

64. Cohen OC, Ismael A, Pawarova B, et al. Longitudinal strain is an independent predictor of survival and response to therapy in patients with systemic AL amyloidosis. *Eur Heart J*. 2021;31:333–341.

65. Milani P, Dispenzieri A, Scott CG, et al. Independent prognostic value of stroke volume index in patients with immunoglobulin light chain amyloidosis. *Circ Cardiovasc Imaging*. 2018;11:e006588.

66. Rubin J, Steidley DE, Carlsson M, et al. Myocardial contraction fraction by M-mode echocardiography is superior to ejection fraction in predicting mortality in transthyretin amyloidosis. *J Card Fail*. 2018;24:504–511.

67. Banypersad SM, Fontana M, Maestrini V, et al. T1 mapping and survival in systemic light-chain amyloidosis. *Eur Heart J*. 2015;36:244–251.

68. Martinez-Naharro A, Kotecha T, Norrington K, et al. Native T1 and extracellular volume in transthyretin amyloidosis. *JACC Cardiovasc Imaging*. 2019;12:810–819.

69. Hutt DF, Fontana M, Burniston M, et al. Prognostic utility of the Perugini grading of ^{99m}Tc-DPD scintigraphy in transthyretin (ATTR) amyloidosis and its relationship with skeletal muscle and soft tissue amyloid. *Eur Heart J Cardiovasc Imaging*. 2017;18:1344–1350.

70. Castano A, Haq M, Narotsky DL, et al. Multicenter study of planar technetium 99m pyrophosphate cardiac imaging: predicting survival for patients with ATTR cardiac amyloidosis. *JAMA Cardiol*. 2016;1:880–889.

71. Lee SP, Suh HY, Park S, et al. Pittsburgh B compound positron emission tomography in patients with AL cardiac amyloidosis. *J Am Coll Cardiol*. 2020;75:380–390.

72. Ioannou A, Massa P, Patel RK, et al. Conventional heart failure therapy in cardiac ATTR amyloidosis. *Eur Heart J*. 2023;44:2893–2907.

73. Porcari A, Cappelli F, Nitsche C, et al. SGLT2 inhibitor therapy in patients with transthyretin amyloid cardiomyopathy. *J Am Coll Cardiol*. 2024;83:2411–2422.

74. Maurer MS, Schwartz JH, Gundapaneni B, et al. Tafamidis treatment for patients with transthyretin amyloid cardiomyopathy. *N Engl J Med*. 2018;379:1007–1016.

75. Ioannou A, Fontana M, Gillmore JD. RNA targeting and gene editing strategies for transthyretin amyloidosis. *BioDrugs*. 2023;37:127–142.

76. Ioannou A. Evolution of disease-modifying therapy for transthyretin cardiac amyloidosis. *Heart Int*. 2024;18:30–37.

77. Ioannou A, Cappelli F, Emdin M, et al. Stratifying disease progression in patients with cardiac ATTR amyloidosis. *J Am Coll Cardiol*. 2024;83:1276–1291.

78. Ioannou A, Fumagalli C, Razvi Y, et al. Prognostic value of a 6-minute walk test in patients with transthyretin cardiac amyloidosis. *J Am Coll Cardiol*. 2024;84:43–58.

79. Ioannou A, Patel R, Gillmore JD, Fontana M. Imaging-guided treatment for cardiac amyloidosis. *Curr Cardiol Rep*. 2022;24:839–850.

80. Rosenblum H, Castano A, Alvarez J, Goldsmith J, Helmke S, Maurer MS. TTR stabilizers are associated with improved survival in patients with transthyretin cardiac amyloidosis. *Circ Heart Fail*. 2018;11:e004769.

81. Siddiqi OK, Mints YY, Berk JL, et al. Diflunisal treatment is associated with improved survival for patients with early stage wild-type transthyretin (ATTR) amyloid cardiomyopathy: the Boston University Amyloidosis Center experience. *Amyloid*. 2022;29:71–78.

82. Koyama J, Minamisawa M, Sekijima Y, et al. Left ventricular deformation and torsion assessed by speckle-tracking echocardiography in patients with mutated transthyretin-associated cardiac amyloidosis and the effect of diflunisal on myocardial function. *Int J Cardiol Heart Vasc*. 2015;9:1.

83. Lohrmann G, Pipilas A, Mussinelli R, et al. Stabilization of cardiac function with diflunisal in transthyretin (ATTR) cardiac amyloidosis. *J Card Fail*. 2020;26:753–759.

84. Shah SJ, Fine N, Garcia-Pavia P, et al. Effect of tafamidis on cardiac function in patients with transthyretin amyloid cardiomyopathy: a post hoc analysis of the ATTR-ACT randomized clinical trial. *JAMA Cardiol*. 2024;9:25–34.

85. Rettl R, Wollenweber T, Duca F, et al. Monitoring tafamidis treatment with quantitative SPECT/CT in transthyretin amyloid cardiomyopathy. *Eur Heart J Cardiovasc Imaging*. 2023;24:1019–1030.

86. Gillmore JD, Judge DP, Cappelli F, et al. Efficacy and safety of acoramidis in transthyretin amyloid cardiomyopathy. *N Engl J Med*. 2024;390:132–142.

87. Razvi Y, Judge DP, Martinez-Naharro A, et al. Effect of acoramidis on myocardial structure and function in transthyretin amyloid cardiomyopathy—insights from the ATTRibute-CM Cardiac Magnetic Resonance (CMR) substudy. *Circ Heart Fail*. 2024;17(12):e012135. https://doi.org/10.1161/CIRCHEARTFAILURE.124.012135

88. Solomon SD, Adams D, Kristen A, et al. Effects of patisiran, an RNA interference therapeutic, on cardiac parameters in patients with hereditary transthyretin-mediated amyloidosis. *Circulation*. 2019;139:431–443.

89. Maurer MS, Kale P, Fontana M, et al. Patisiran treatment in patients with transthyretin cardiac amyloidosis. *N Engl J Med*. 2023;389:1553–1565.

90. Adams D, Tournev IL, Taylor MS, et al. Efficacy and safety of vutrisiran for patients with hereditary transthyretin-mediated amyloidosis with polyneuropathy: a randomized clinical trial. *Amyloid*. 2022;30:1–9.

91. Ioannou A, Fontana M, Gillmore JD. Patisiran for the treatment of transthyretin-mediated amyloidosis with cardiomyopathy. *Heart Int*. 2023;17:27–35.

92. Fontana M, Berk JL, Gillmore JD, et al. Vutrisiran in patients with transthyretin amyloidosis with cardiomyopathy. *N Engl J Med*. 2025;392:33–44. https://doi.org/10.1056/NEJMoa2409134

93. Coelho T, Marques W, Dasgupta NR, et al. Eplontersen for hereditary transthyretin amyloidosis with polyneuropathy. *JAMA*. 2023;330:1448–1458.

94. Masri A, Maurer MS, Claggett BL, et al. Effect of eplontersen on cardiac structure and function in patients with hereditary transthyretin amyloidosis. *J Card Fail*. 2024;30:973–980.

95. Gillmore JD, Gane E, Taubel J, et al. CRISPR-Cas9 in vivo gene editing for transthyretin amyloidosis. *N Engl J Med*. 2021;385:493–502.

96. Fontana M, Gilbertson J, Verona G, et al. Antibody-associated reversal of ATTR amyloidosis-related cardiomyopathy. *N Engl J Med*. 2023;388:2199–2201.

97. Garcia-Pavia P, aus dem Siepen F, Donal E, et al. Phase 1 trial of antibody NI006 for depletion of cardiac transthyretin amyloid. *N Engl J Med*. 2023;389:239–250.

98. Prothena Reports Positive 9 Month Results from Phase 1 Long-term Extension Study of PRX004, the First Investigational Anti-Amyloid Immunotherapy for the Treatment of ATTR Amyloidosis. BioSpace. Accessed February 25, 2024. https://www.biospace.com/article/releases/prothena-reports-positive-9-month-results-from-phase-1-long-term-extension-study-of-prx004-the-first-investigational-anti-amyloid-immunotherapy-for-the-treatment-of-attr-amyloidosis/

99. Wall J, Klein M, Guthrie S, et al. The Peptide Fusion Immunoglobulin, AT-02, Exhibits Highly Potent Pan-Amyloid Reactivity And Immunomodulation. *J Card Fail*. 2024;30:210.

100. Palladini G, Dispenzieri A, Gertz MA, et al. New criteria for response to treatment in immunoglobulin light chain amyloidosis based on free light chain measurement and cardiac biomarkers: impact on survival outcomes. *J Clin Oncol*. 2012;30:4541–4549.

101. Edwards CV, Rao N, Bhutani D, et al. Phase 1a/b study of monoclonal antibody CAEL-101 (11-1F4) in patients with AL amyloidosis. *Blood*. 2021;138:2632–2641.

102. Gertz MA, Cohen AD, Comenzo RL, et al. Birtamimab plus standard of care in light-chain amyloidosis: the phase 3 randomized placebo-controlled VITAL trial. *Blood*. 2023;142:1208–1218.

103. Salinaro F, Meier-Ewert HK, Miller EJ, et al. Longitudinal systolic strain, cardiac function improvement, and survival following treatment of light-chain (AL) cardiac amyloidosis. *Eur Heart J Cardiovasc Imaging*. 2017;18:1057–1064.

104. Martinez-Naharro A, Patel R, Kotecha T, et al. Cardiovascular magnetic resonance in light-chain amyloidosis to guide treatment. *Eur Heart J*. 2022;00:1–14.

105. Ioannou A, Patel RK, Martinez-Naharro A, et al. Tracking treatment response in cardiac light-chain amyloidosis with native T1 mapping. *JAMA Cardiol*. 2023;8:848–852.

KEY WORDS Cardiac amyloidosis, systemic light-chain amyloidosis, transthyretin amyloidosis